Disease-modifying effects of sodium selenate in a model of drug-resistant, temporal lobe epilepsy.

Authors: Pablo M. Casillas-Espinosa[1,2,4]*, Alison Anderson[1,2], Anna Harutyunyan[1,2], Crystal Li[2], Jiyoon Lee[1], Emma L. Braine[1,2], Rhys D. Brady[1,2], Mujun Sun[2], Cheng Huang[3], Christopher K. Barlow[3], Anup D. Shah[3], Ralf B. Schittenhelm[3], Richelle Mychasiuk[2], Nigel C. Jones[1,2], Sandy R. Shultz[1,2], Terence J. O'Brien[1,2,4]*.

Abstract

There are no pharmacological disease-modifying treatments that can mitigate the seizures and comorbidities associated with established chronic temporal lobe epilepsy (TLE). This study evaluated the effect of sodium selenate in the post-status epilepticus (SE) rat model of chronic drug resistant TLE. Wistar rats underwent kainic acid-induced SE or sham. Ten-weeks post-SE, rats were randomly assigned to receive either sodium selenate, levetiracetam, or vehicle treatments continuously for 4 weeks. To evaluate the effects of the treatments, 1 week of continuous video-EEG was acquired before, during, and 4, 8 weeks post-treatment, followed by behavioral tests. Targeted and untargeted proteomics and metabolomics were performed on post-mortem brain tissue to identify potential pathways associated with modified disease outcomes. Telomere length was investigated as a novel surrogate marker of disease severity. Sodium selenate treatment was able to mitigate disease severity, reducing the number of spontaneous seizures ($p< 0.05$), cognitive dysfunction ($p< 0.05$ in both novel object placement and recognition tasks), and sensorimotor deficits ($p< 0.01$) 8 weeks post-treatment cessation. Moreover, increased protein phosphatase 2A (PP2A) expression, reduced hyperphosphorylated

tau, and reversed telomere length shortening caused by SE ($p < 0.05$). Network medicine integration of multi-omics/ pre-clinical outcomes identified protein-metabolite modules positively correlated with the TLE phenotype. Our results provide evidence that treatment with sodium selenate results in a sustained disease modifying effect in chronically epileptic rats in the post-KA SE model of TLE, including improved comorbid learning and memory deficits.

Author affiliations:

[1] Department of Medicine, The Royal Melbourne Hospital, The University of Melbourne, Royal Parade, Parkville, Victoria 3050, Australia

[2] Department of Neuroscience, Central Clinical School, Monash University, Melbourne, Victoria, 3004 Victoria, Australia.

[3]Monash Proteomics & Metabolomics Facility and Monash Biomedicine Discovery Institute, Monash University, Clayton, Victoria 3800, Australia

[4] Department of Neurology, The Alfred Hospital, Commercial Road, Melbourne, Victoria, 3004 Victoria, Australia.

* Denotes corresponding authors

Correspondence to:

Dr. Pablo M. Casillas-Espinosa

Department of Neuroscience, Central Clinical School, Monash University, Melbourne, Victoria, 3004 Victoria, Australia

Email: pablo.casillas-espinosa@monash.edu

Phone: +61 3 9903 8669

Prof. Terence J. O'Brien,

Department of Neuroscience, Central Clinical School, Monash University, Melbourne, Victoria, 3004 Victoria, Australia

Email: terence.obrien@monash.edu

Phone: +61 3 99030855

Keywords: disease-modification, kainic acid, post-SE model, neuropharmacology, behavior, cognition, comorbidities, pre-clinical drug trial

Abbreviations: ASMs = anti-seizure medications; BT = beam test; DMT = disease-modifying treatment; EPM = elevated plus maze; FGRF = fibroblast growth factor receptors; gDNA = genomic DNA; IGRF = insulin-like growth factor receptor; KA = kainic acid; MWM = Morris water maze; NMDA = N-methyl-D-aspartate; NOP = Novel object placement; NOR = Novel Object Recognition; OF = Open field; PADOG = Pathway Analysis with Down-weighting of Overlapping Genes; PCA = principal component analysis; PI-3K = phosphatidylinositol 3-kinase; PLS-DA = partial least square-discriminant analysis; PP2A = protein phosphatase 2A; RIPA = radioimmunoprecipitation assay; SE = status epilepticus; TL = telomere length; TLE = Temporal lobe epilepsy; WGCNA = weighted correlation network

Introduction

Temporal lobe epilepsy (TLE) is the most common form of drug-resistant epilepsy in adults, and is frequently accompanied by disabling neuropsychiatric and cognitive comorbidities (Hermann *et al.*, 2008; Hermann *et al.*, 2000; Kwan *et al.*, 2011; Sharma *et al.*, 2007; Tellez Zenteno *et al.*, 2007). People with epilepsy are often required to take multiple anti-seizure medications (ASMs) in an attempt to control their seizures. However, these treatments are often ineffective at controlling seizures in more than 30% of the cases(Hermann *et al.*, 2008; Hermann *et al.*, 2000; Kwan *et al.*, 2011; Sharma *et al.*, 2007; Tellez Zenteno *et al.*, 2007), and can cause significant adverse side effects (Alonso-Vanegas *et al.*, 2013; Perucca and Gilliam, 2012; Taylor *et al.*, 2011). Current ASMs are merely symptomatic and do not mitigate the severity, progression or outcome of the epilepsy, and if the patient ceases the medication their seizures are just as severe and frequent as if the person has never took the medication in the first place (Simonato *et al.*, 2014). Despite decades of research and development, the more than 20 new ASMs that have been introduced to clinical practice have failed to reduce the proportion of people with epilepsy who have drug-resistant seizures (Chen *et al.*, 2018). Moreover, the cognitive and neuropsychiatric comorbidities that are prevalent in these patients remain difficult to treat and are not improved by the ASM treatment (Hinnell *et al.*, 2010; Valente and Busatto Filho, 2013).

Animal studies have identified compounds potentially capable of delaying epileptogenesis (i.e. the process by which a non-epileptic brain turns into an epileptic one), but to date, these have only been demonstrated to be effective when the treatment is initiated early in the disease process (i.e. immediately after the brain insult) (Casillas-Espinosa *et al.*, 2019b; Liu *et al.*, 2016; Pauletti *et al.*, 2019; Rizzi *et al.*, 2019; Zeng *et al.*, 2009; Zhong Huang *et al.*, 2019). Because the majority of TLE patients already have established epilepsy when they present to the clinic(Foster *et al.*, 2019), and there are no reliable biomarkers to predict who will develop

TLE, this treatment strategy has limited clinical utility (Simonato *et al.*, 2021). Surgical resection of the epileptogenic zone is the only disease-modifying treatment (DMT) currently available, which may convert drug-resistant TLE into drug-responsive TLE in selected patients. However, <5% of patients with drug resistant epilepsy are suitable for resective epilepsy surgery, and it is invasive with significant potential risks and is unsuccessful in controlling seizures in 20 – 40% of patients (Téllez-Zenteno *et al.*, 2005). Thus, there is a compelling need to identify medical DMTs that are effective in patients with chronic TLE. (O'Brien *et al.*, 2013; Sharma *et al.*, 2007; Simonato *et al.*, 2013).

Hyperphosphorylated tau (h-tau) is a neuropathological hallmark of several neurodegenerative conditions and has recently been implicated in epileptogenesis (Casillas-Espinosa, 2020; Ittner and Götz, 2011; Johnstone *et al.*, 2015; Liu *et al.*, 2016; Sen *et al.*, 2007; Shultz *et al.*, 2015; Thom *et al.*, 2011; van Eersel *et al.*, 2010). For example, hyperphosphorylated tau (h-tau) is present in the brains of rodents with TLE, (Corcoran *et al.*, 2010b; Jones *et al.*, 2012; Shultz *et al.*, 2015) and deposits of h-tau have been identified in surgically resected tissue from patients with drug-resistant epilepsy (Puvenna *et al.*, 2016; Sanchez *et al.*, 2018; Sen *et al.*, 2007; Tai *et al.*, 2016; Thom *et al.*, 2011). The primary tau phosphatase in the brain (i.e. an enzyme that dephosphorylates tau) is protein phosphatase 2A (PP2A)(Corcoran *et al.*, 2010a), a heterotrimer consisting of a catalytic C subunit, a scaffold A subunit and a regulatory B subunit with variable isoforms (Janssens and Goris, 2001). In several models of epilepsy, activation of PP2A with sodium selenate has been shown to reduce h-tau, and early treatment imparts anti-epileptogenic effects, while also reducing behavioral deficits associated with the epilepsy (Liu *et al.*, 2016). However, whether pharmacological intervention with sodium selenate in chronic epileptic animals is a DMT remains to be determined. Therefore, this study investigated the effect of sodium selenate treatment on epileptic and behavioral outcomes, as well as multi-omics network medicine and bioinformatics approaches to uncover relevant molecular

pathways, in chronically epileptic rats. We used the well-validated kainic acid (KA) post- post-status epilepticus (SE) model of TLE, where animals develop resistance to drug treatment, behavioral, cognitive, and sensorimotor comorbidities analogous to human drug-resistant TLE (Casillas-Espinosa *et al.*, 2019b; Thomson *et al.*, 2020).

Materials and Methods

Animals

Eleven-week-old male Wistar rats were used in all of the experiments. All procedures were approved by the Florey Animal Ethics Committee (ethics number 16-042-UM) and adhered to the Australian code for the care and use of animals for scientific purposes. All the experiments were conducted by researchers blinded to the experimental conditions.

Sample size

Power analyses based on our previously published KA-induced post-SE rat model studies (Casillas-Espinosa *et al.*, 2019b; Liu *et al.*, 2016), indicated that an n=8 per group was required to detect a 30% difference between the treatment groups considering α=0.05 and power=95%.

Modified kainic acid-induced post-status epilepticus experimental protocol

The KA-induced post-SE model was used to evaluate the disease-modifying effects of sodium selenate. Figure 1 summarizes the experimental paradigm for the current study.

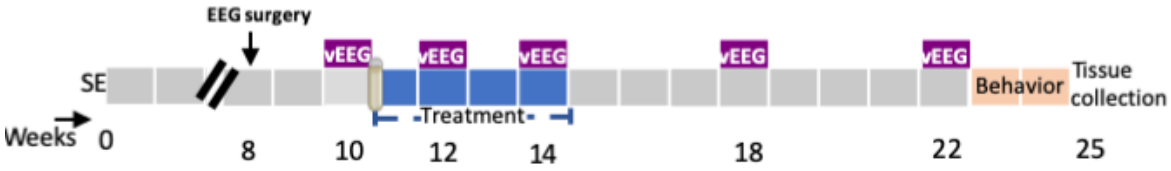

Figure 1: Experimental protocol in the post-status epilepticus model of temporal lobe epilepsy (TLE). SE =KA-induced status epilepticus, vEEG = video-electroencephalogram; weeks = weeks post SE.

The animals where individually housed with alternating 12-hour cycles of light and dark (lights on at 07:00h). Food and water were provided *ad libitum* for the whole duration of the study. A

repeated low dose KA administration protocol was used (Bhandare *et al.*, 2017; Casillas-Espinosa *et al.*, 2019b). Rats were injected i.p. with an initial dose of KA 7.5 mg/kg. Animals were monitored for behavioral seizures based on the Racine scale (Racine, 1972). If no continuous seizure activity was observed with at least five class 5 seizure of Racine, another i.p. dose of 5 mg/kg followed by 2.5 mg/kg doses of KA were administered up to a maximum of 20 mg/kg (Brady *et al.*, 2019). An animal was eliminated from the experiment if it didn't show a stable self-sustained SE after a maximum KA dose. Shams were handled identically but received saline injections instead of KA. After four hours of sustained EEG and behavioral seizures the animals were given diazepam (5 mg/kg/dose) to stop the SE (Bhandare *et al.*, 2017; Casillas-Espinosa *et al.*, 2019b).

EEG electrode implantation surgery

Nine weeks after the induction of SE, rats were anesthetized with isoflurane (Ceva isoflurane, Piramal Enterprises Limited, India) and EEG Surgery was performed under aseptic technique as previously described (Casillas-Espinosa *et al.*, 2019a). (Casillas Espinosa *et al.*, 2015). Four burr holes were drilled through the skull without penetrating the dura, one on each side of the frontoparietal region (AP: ±1.7; ML: -2.5), two to each side of the temporal region (AP: ±5. 6; ML: left 2.5) anterior to lambda and four epidural stainless-steel screw recording electrodes (EM12/20/SPC, Plastics One Inc) were screwed into the burr holes. Ground and reference electrodes were implanted on each side of the parietal bone above the cerebellum (Casillas Espinosa *et al.*, 2019; Santana-Gomez *et al.*, 2019) and were secured using dental cement (VX-SC1000GVD5/VX-SC1000GMLLQ, Vertex, Australia) around the electrodes and over the skull. Buprenorphine (0.05 mg/kg, Indivior Australia) was used as an analgesic(Casillas Espinosa *et al.*, 2019).

Video-EEG acquisition

Ten weeks after the induction of SE, animals were connected using cables (M12C-363, Plastics One Inc, Australia) (Casillas-Espinosa *et al.*, 2019b). vEEG recordings were acquired using Profusion 3 software (Compumedics, Australia) unfiltered and digitized at 512Hz.

Pre-treatment seizure analyses screening

All vEEG recordings were screened for seizures using Assyst, a semi-automated seizure detection software (Assyst, Australia) (Casillas-Espinosa *et al.*, 2019a). Seizure events were visually confirmed using Profusion 3 software by two blinded independent experts. A seizure was defined as an episode of rhythmic spiking activity that was three times the baseline amplitude and a frequency > 3 Hz that lasted at least 10 s; the end of a seizure was determined as the last spike (Brady *et al.*, 2019; Casillas-Espinosa *et al.*, 2019a; Casillas-Espinosa *et al.*, 2019b; Ndode Ekane *et al.*, 2019; Pitkanen *et al.*, 2005; Van Nieuwenhuyse *et al.*, 2015b). The average number of seizures per day, average seizure duration and seizure class (i.e., severity, Racine scale) were analyzed (Brady *et al.*, 2019; Casillas-Espinosa *et al.*, 2019b). Animals that did not have 2 or more seizures during the week of baseline video-EEG (vEEG) were discarded from the experiments.

Group allocation and osmotic pump implantation surgery

Shams (n=11); and post-SE rats that had seizures during the pre-treatment seizure screening week were randomly allocated to one of the four treatment groups: post-SE + vehicle (n=12), post-SE + sodium selenate (n=12), post-SE + levetiracetam (n=12). Subcutaneous osmotic pumps (2ML4, delivery rate 2.5 µl/h, Alzet, Cupertino, CA, USA) that delivered sodium selenate (1 mg/kg/day; SKU: 71948, Sigma-Aldrich, Castle Hill, Australia), levetiracetam (200 mg/kg/day; Angene, London, England)) or vehicle (saline 0.9%) were implanted and treatment

was continuously delivered for four weeks (Casillas-Espinosa *et al.*, 2019b; Li *et al.*, 2018). Sodium selenate and levetiracetam doses were selected based on previous studies (Brandt *et al.*, 2007; Casillas-Espinosa *et al.*, 2019b; Li *et al.*, 2018; Loscher and Honack, 1993; Loscher *et al.*, 1998; Shultz *et al.*, 2015).

vEEG analysis to evaluate disease modification in chronic TLE

To evaluate the disease modifying effects of the different treatments, animals underwent seven days of continuous vEEG recordings during the second and fourth week of treatment, and during the week four and eight post-washout (Figure 1). A washout period of eight weeks was chosen to provide a long-term monitoring of the disease-modifying effects of the treatments (Barker-Haliski *et al.*, 2015; Casillas-Espinosa *et al.*, 2019b). Seizure duration and class were considered from only the animals that presented with spontaneous seizures. vEEG analysis was performed in a blinded manner and confirmed by two different observers as described above.

Behavioral tests

All behavioral tests were performed in a light-controlled (~110 lux), closed, quiet and clean room between 9 am and 5 pm. The animals had at least 1h to acclimatize to the room before the start of any of the behavioral tests. Behavioral testing was performed in a blinded manner to the treatment groups. All of the behavioral tests were video recorded for future analysis. Open field (OF), elevated plus maze (EPM), Novel object placement (NOP), Novel Object Recognition (NOR), beam test (BT), and Morris water maze (MWM) sessions were filmed using a digital camera mounted above the center of the arena, which was connected to a computer for the recording and objective analysis of digitized behavioral tests (Ethovision 3.0.15, Noldus) and were conducted as previously described (Bao *et al.*, 2012; Broadbent *et al.*, 2004; Casillas-Espinosa *et al.*, 2019b; Johnstone *et al.*, 2015; Jones *et al.*, 2008; Kolb and

Whishaw, 1985; Morris, 1984; Pearson *et al.*, 2014; Shultz *et al.*, 2015).

Elevated plus maze (EPM)

The EPM is a custom-made black acrylic arena in the shape of a plus, with one opposing pair of arms enclosed by 30 cm high walls (closed arms) and the other opposing arms without any enclosure (open arms). Each arm is 13 cm wide and 43.5 cm long, and the maze is elevated 60 cm above the floor. The rat was placed in the center of the EPM, and its behavior was monitored over 5 minutes (Casillas-Espinosa *et al.*, 2019b; Johnstone *et al.*, 2015; Jones *et al.*, 2008). The EPM was wiped clean between each animal. The distance travelled, number of entries into the open and closed arms, and the total time spent in each arm during the trial were recorded.

Open field (OF)

The OF is a 100 cm diameter circular arena, with an inner circle arena of 66 cm of diameter that was virtually defined using the Ethovision software. For each test, the rat is placed gently into the center of the field and its behavioral activity is monitored for 10 min. The distance travelled as well as the entries and time spent in the inner circle were recorded (Casillas-Espinosa *et al.*, 2019b; Johnstone *et al.*, 2015; Jones *et al.*, 2008).

Novel object placement object (NOP)

The test took place in the same circular arena used for the OF test, and consisted of two phases, a learning phase and a memory (testing) phase. During the learning phase, animals were placed into the behavioral arena for a period of 5 minutes and allowed to explore two identical stimulus objects (plastic green trees) before being placed back into the home cage. 15 minutes after the first stage, the animal was re-introduced to the arena, except that during the memory phase, one of the objects was displaced to a novel spatial location. In the first stage, two identical objects (plastic green tree) were each placed at the center of two adjacent quadrants of the circular

arena and rats were allowed to freely explore the arena for another 5 minutes(Broadbent *et al.*, 2004; Pearson *et al.*, 2014). Animals were assessed on the time spent around the objects, and percentage of time the animal investigated the object in a novel location.

Novel object recognition (NOR)

The first phase of the test was identical to the learning phase of the NOP test. However, in the second stage of the NOR test, commencing 15 minutes after the first stage, one of the objects was replaced by a novel and unfamiliar object (plastic red car), which was placed in the exact same position as one of the original objects and the animal was allowed to explore the arena for 5 minutes(Broadbent *et al.*, 2004; Pearson *et al.*, 2014). Animals were assessed on the time spent around the objects, and percentage of time the animal investigated the novel object.

Beam task (BT)

The beam task (BT) is used to assess sensorimotor function (Bao *et al.*, 2012; Kolb and Whishaw, 1985). The test was divided in a training and a testing session. During the training session rats underwent five trials to traverse a 100 cm long beam with a width of 4 cm, and a further five trials to traverse a 100 cm long beam with a width of 2 cm. Twenty-four hours after the training session, the BT testing session was performed and consisted of 10 trials on the 2 cm wide, 100 cm long beam. Each trial began with the rat being placed at one end of the beam and ended when the animal successfully traversed a distance of 100 cm. A maximum of 60 s was allowed for each trial. If the rat fell off the beam it was given a time of 60 s. Each trial was recorded by a camera, and traverse time and the number of slips and falls were used as measures of sensorimotor function (Shultz *et al.*, 2015).

Morris water maze (MWM)

The MWM is a circular black PVC plastic pool of 160 cm diameter which is filled to a depth of 2.5 cm above a 10 cm diameter hidden platform water at 25 ± 1˚C (Casillas-Espinosa *et al.*, 2019b; Morris, 1984; Shultz *et al.*, 2015). The platform is located in the center of the South-West quadrant. Visual cues are placed in the main four cardinal points, consisting of large black and white symbols that serve as orientation landmarks for the rats. The test was performed over two days in an acquisition (day 1) and reversal (day 2) session. The acquisition session consisted of 10 trials. A trail begins by placing gently the rat in the pool, facing the pool wall, and ended when the rat stands on the platform for at least 3 seconds, or when 90 seconds had elapsed. Each trial began at one of four pool walls start locations (North, South, East, or West) according to a pseudo-random schedule of start locations that prevented repeated sequential starts from the same location (Liu *et al.*, 2016; Shultz *et al.*, 2015). The reversal session of the water maze was completed 24 h after acquisition. The procedures were identical to those of the acquisition session except that the hidden platform was now located in the north-west quadrant of the pool. The latency to find the escape platform, speed and strategic path used by the animal to locate the platform are recorded. Search time was used as measures of spatial orientation and memory (Bao *et al.*, 2012; Casillas-Espinosa *et al.*, 2019b; Morris, 1989; Whishaw and Jarrard, 1995). Swim speed (cm/s) was used as a measure of motor ability (Bao *et al.*, 2012).

Sucrose preference test (SPT)

The sucrose preference test (SPT) is a well-validated measure of depression/anhedonia in rats (Casillas-Espinosa *et al.*, 2019b; Jones *et al.*, 2008). The SPT was used to evaluate the effects of the treatments to modify the depressive-like behavior seen in post-SE rats. The sucrose preference was calculated as the percentage of the sucrose solution consumed from the total volume (of both sucrose and water). The animals remained in their same home cage during the testing. One hour before the start of the test, the animals were given up to 0.5 ml of the testing 2% sucrose to ensure that the animals would drink the sucrose solution. The animals were

presented with two bottles, one filled with water and the other one filled with 2% sucrose in water for 24 hours(Casillas-Espinosa *et al.*, 2019b). Bottle position was randomized to avoid position preference (Casillas-Espinosa *et al.*, 2019b; Jones *et al.*, 2008; Sarkisova *et al.*, 2003). Total fluid intake and percentage preference for sucrose were recorded. The results of the sucrose preference test are presented in Supplementary Figure A1.

Tissue collection

Seven days after the last behavioral test, the animals were anesthetized using 5% isoflurane, and were culled using a lethal dose of intraperitoneal Lethabarb (150mg/kg IP; pentobarbitone sodium; Virbac, Australia)(Casillas-Espinosa *et al.*, 2019b). Tissue was taken from each rat's ear and stored at −80 °C for telomere length (TL) analysis (Hehar and Mychasiuk, 2016). Using the Rat Brain Atlas as a reference (Paxinos and Watson, 1982), the hippocampus and somatosensory cortex from (n=3) rats per treatment cohort were rapidly dissected, flash frozen with liquid nitrogen and stored at −80 °C for untargeted proteomics, metabolomics, and western blot studies.

Data-Independent proteomic analysis

Frozen hippocampus and somatosensory cortex samples were homogenized in liquid nitrogen and lysed in 4%SDS, 100mM HEPES, pH8.5, which was then heated at 95°C for 5 min and sonicated 3 times for 10 sec each at an amplitude of 10 µm. The lysate was clarified by centrifuging at 16 000 g for 10 minutes and protein concentration was determined by Pierce™ BCA Protein Assay Kit (Thermo). Equal amount of protein was denatured and alkylated using Tris(2-carboxyethyl)-phosphine-hydrochloride (TCEP) and 2-Chloroacetamide (CAA) at a final concentration of 10 mM and 40 mM, respectively, and incubated at 95°C for 5 min. SDS was removed by chloroform/methanol. Sequencing grade trypsin was added at an enzyme to protein ratio of 1:100 and the reaction was incubated overnight at 37°C. The digestion reaction

was stopped by adding formic acid to a concentration of 1%. The peptides were cleaned with BondElut Omix Tips (Agilent) and concentrated in a vacuum concentrator prior to analysis by mass spectrometry.

Using a Dionex UltiMate 3000 RSLCnano system equipped with a Dionex UltiMate 3000 RS autosampler, the samples were loaded via an Acclaim PepMap 100 trap column (100 µm x 2 cm, nanoViper, C18, 5 µm, 100å; Thermo Scientific) onto an Acclaim PepMap RSLC analytical column (75 µm x 50 cm, nanoViper, C18, 2 µm, 100å; Thermo Scientific). The peptides were separated by increasing concentrations of 80% ACN / 0.1% FA at a flow of 250 nl/min for 158 min and analyzed with a QExactive HF mass spectrometer (Thermo Scientific) operated in data-independent acquisition (DIA) mode. Sixty sequential DIA windows with an isolation width of 10 m/z have been acquired between 375 - 975 m/z (resolution: 15.000; AGC target: 2e5; maximum IT: 9 ms; HCD Collision energy: 27%) following a full ms1 scan (resolution: 60.000; AGC target: 3e6; maximum IT: 54 ms; scan range: 375-1575 m/z). The acquired DIA data have been evaluated in Spectronaut 13 Laika (Biognosys) using an existing, in-house generated spectral library derived from rat brain samples.

Untargeted metabolomics studies

The same frozen hippocampal and somatosensory cortex samples used for proteomics were cryogenically pulverized (cryopulverization) using a 12-well biopulverizer (BioSpec Products, OK USA Part number 59012MS) according to the manufacturer's instructions. The frozen tissue powder was then weighed and extracted in 20 µL of extraction solvent (0°C) per mg of tissue. The mixture was then briefly vortexed before sonication in an ice-water bath for 10 minutes followed by centrifugation (20,000 rcf, 4°C, 10 minutes). The supernatant was then transferred to a mass spectrometry vial for LC-MS analysis. The extraction solvent consisted of 2:6:1 CHCl3:MeOH:H2O v/v/v with 2 µM CHAPS, CAPS, PIPES and TRIS as internal

standards.

Plasma (25 µL) was extracted by addition of 200 µL of 1:1 acetonitrile:MeOH v/v with 2 µM CHAPS, CAPS, PIPES and TRIS as internal standards at 0°C. Samples were then mixed on a vortex mixer for 45 cycles 20 sec each at 4°C after which they were centrifuged (20,000 rcf, 4°C, 15 min) and the supernatant then transferred to a mass spectrometry vial for LC-MS analysis.

For LC−MS analysis, samples were analyzed by hydrophilic interaction liquid chromatography coupled to high-resolution mass spectrometry (LC−MS) (Creek *et al.*, 2012; Srivastava *et al.*, 2017). In brief, the chromatography utilized a ZIC-pHILIC column (column temperature 25 °C) with a gradient elution of 20 mM ammonium carbonate (A) and acetonitrile (B) (linear gradient time-%B as follows: 0 min-80%, 15 min-50%, 18 min-5%, 21 min-5%, 24 min-80%, 32 min-80%) on a Dionex RSLC3000 UHPLC (Thermo). The flow rate was maintained at 300 µL/min. Samples were kept at 4 °C in the autosampler and 10 µL injected for analysis. The mass spectrometry was performed at 35 000 resolution (accuracy calibrated to <1 ppm) on a Q-Exactive Orbitrap MS (Thermo) operating in rapid switching positive (4 kV) and negative (−3.5 kV) mode electrospray ionization (capillary temperature 300 °C; sheath gas 50; Aux gas 20; sweep gas 2; probe temp 120 °C). All samples were analyzed in randomized order and with pooled quality control samples analyzed regularly throughout the batch to confirm reproducibility. Approximately 300 metabolite standards, including all reported amino acids, were analyzed immediately preceding the batch to determine accurate retention times to confirm metabolite identification.

For data analysis, untargeted metabolomics data were analyzed using the IDEOM (version 20) workflow with default parameters (Creek *et al.*, 2012). In brief, this involved peak picking with

XCMS (Tautenhahn *et al.*, 2008), peak alignment and filtering with mzMatch (Scheltema *et al.*, 2011) and further filtering, metabolite identification, and comparative analysis with IDEOM.

Proteomic and metabolomic data analysis

The proteomic and metabolomic mass-spectroscopy data from the somatosensory cortex and hippocampus of rats treated with selenate, levetiracetam, vehicle and sham were tabulated into spectral peak intensity values followed by log2 transformation and unit-variance scaled. The missing values were omitted by replacing them with background signal. One-way ANOVA and Tukey's HSD were employed to identify differences in metabolite and protein abundance between levetiracetam, selenate, vehicle and sham groups. A false discovery rate of FDR<0.05 was deemed significant. In addition to the univariate analysis, multivariate analysis in the form of principal component analysis (PCA) and partial least square-discriminant analysis (PLS-DA) was performed in order to identify the metabolites and proteins driving the separation between treatment groups. Metabolite set enrichment analysis (MSEA) was performed between all pairs of groups via quantitative enrichment module of MetaboAnalyst 5.0 web tool (Pang *et al.*, 2021) for the metabolomic data.

Quantitative gene set enrichment analysis was performed between all pairs of treatment groups via Pathway Analysis with Down-weighting of Overlapping Genes (PADOG) module of Reactome web-based tool (Fabregat *et al.*, 2018; Jassal *et al.*, 2020) for proteomic data. PADOG is a weighted gene/protein set analysis method that down-weighs genes/proteins that are present in many pathways thus preventing their exaggerated significance. Pathways with FDR of < 0.05 were considered differentially regulated.

Multi-omic correlation network analysis, module detection and functional annotation

We employed early integration and weighted correlation network analysis (WGCNA) (Zhang *et al.*, 2013) methods to characterize the proteome and metabolome of SE rats. Correlation-based networks of proteins and metabolites were constructed, which were then clustered into modules and functionally annotated through pathway enrichment analysis.

To integrate the proteomic and metabolomic data for network analysis, we unit variance scaled and concatenated the normalized proteomic and metabolomic data into a single matrix. Unit variance scaling uses standard deviation as the scaling factor; thus, the resultant integrated data can be analyzed on the basis of correlations (Zhang *et al.*, 2013). Correlation-based multi-omics networks were then constructed for all treatment groups by employing the framework of WGCNA using the WGCNA R package (Langfelder and Horvath, 2008). Briefly, an adjacency matrix was constructed reflecting the pairwise Pearson correlations between all detected proteins and metabolites across all samples. The correlation network was then built based on the adjacency matrix, where each node corresponds to a single metabolite or protein, and the edges between the nodes represent the correlation between the relative abundance of the given metabolite/protein across all samples. A clustering algorithm was employed to identify metabolite/protein modules (labeled by color), which then were functionally annotated through joint pathway enrichment analysis (Pang *et al.*, 2021) of all metabolites/proteins constituting each module. The Spearman correlation of modules to clinical traits such as average seizure class, telomere length and cognitive performance was examined.

Targeted protein expression using automated Capillary Western Blots

Capillary Western blots were used to assess protein expression of hyperphosphorylated tau (h-tau), total tau and PP2A. A portion of the frozen somatosensory cortex\tissue was homogenized in radioimmunoprecipitation assay (RIPA) buffer with protease and phosphatase inhibitors (SigmaFast, S8820, Sigma-Aldrich, USA and PhosStop, 4906837001, Sigma-Aldrich, USA)

The protein concentration of the lysates was quantified using a BCA Protein Assay Kit (Thermo Scientific Pierce Biotechnology, USA) and Benchmark Plus Microplate Spectrophotometer (Bio-Rad, Hercules, United States). Capillary Western analyses were performed using the Wes Protein Simple Western System (12-kDA Wes separation module kit, SWM-W001, ProteinSimple, United States) according to the manufacturer's instructions.\Individual assays were performed for total tau (Tau-5, # 577801, Millipore, Australia, 1:50), h-tau (p-Ser202/Thr205-tau (AT8), # MN1020, ThermoFisher Scientific, Australia, 1:200), PP2A subunit B (#05-592, Millipore, Australia, 1:200) and Glyceraldehyde 3-phosphate dehydrogenase (GAPDH; 1:200, Santa Cruz Biotechnology #sc-47724, USA) was used as loading control. H-tau was determined as the ratio of phosphorylated tau (AT8) relative to total tau (tau 5) (Shultz *et al.*, 2015) (Liu *et al.*, 2016). Raw ir data is expressed as the percentage of the average of controls (Liu *et al.*, 2016). All the semi-automated western blot procedures were conducted by an experimenter blinded to experimental conditions.

Telomere length analysis

Ear samples (5-7/group were collected at the end of the study). The Qiagen DNA Micro kit (Qiagen, Germany) was used to extract genomic DNA (gDNA) as described in (Cawthon, 2002; Hehar and Mychasiuk, 2016). gDNA samples had mean 260/230 and 260/280 spectral ratios of 2.24 and 1.90, respectively. TL analysis was conducted on all diluted DNA samples (20 ng/µL) using a similar protocol to that previously described (Sun *et al.*, 2019). RT-qPCR reactions were conducted by adding 1 µL DNA, 1 × SYBR Green FastMix with Rox and primers so that the total volume in each well was 20 µL. Each reaction was performed in duplicate, including no template controls (NTC) to ensure that the reactions were not contaminated. Primer final concentrations were (forward/reverse): 270 nM/900 nM for Tel; and 300 nM/500 nM for 36B4 (Hehar and Mychasiuk, 2016). Absolute quantitative PCR was used

to determine the ratio of telomeres to a single copy gene (36B4), calculated as $[2Ct(telomeres) / 2Ct(36B4)]-1 = -2-\Delta Ct$. This was then used in the following formula to determine TL: $TL = 1910.5 * (-2-\Delta Ct) + 4157$ (Cawthon, 2002; Hehar and Mychasiuk, 2016; Sun *et al.*, 2019).

Statistical analysis

All EEG parameters were compared using with a two-way repeated measure ANOVA, separating the periods during and following the treatment period into different analyses (Dezsi *et al.*, 2013). During treatment, the between subject factor was treatment, and the within subject factor was timepoint of recording. After treatment (i.e., drug washout), ANOVA was used to assess whether seizures were modified following the removal of treatment, using the same parameters as above. *Post hoc* analyses were used to test for multiple comparisons and control for chance. For the seizure data, Tukey's *post hoc* was used. MWM was also analyzed, using two-repeated measures ANOVA with Dunnett's *post hoc*. Data was analyzed for normality using the Shapiro-Wilk test. Normally distributed, (OF, EPM, BT, TL and western blot) data was analyzed using one-way ANOVA with Tukey *post hoc*. For the data that did not fit a normal or Gaussian distribution (NPO, NOR, SPT and FST), a Kruskal-Wallis with Dunn's *post hoc* was used instead. Correlation studies were performed on data that was significantly different between the experimental groups. Pearson correlation were performed between the average number of seizures per day, MWM, BT and TL. Spearman correlation was performed between average number of seizures per day, NPO and NOR. The analyzed data was reported as the mean and standard error of the mean (SEM) with statistical significance set at $p<0.05$. All the statistical comparisons were done using GraphPad Prism 9 (GraphPad Software, Inc. USA).

Data availability

Data has been deposited in Dryad https://doi.org/10.5061/dryad.37pvmcvnd

Results

This study evaluated the effect of sodium selenate on established TLE, using the post-SE model of drug resistant TLE. Ten-weeks post-SE, chronically epileptic rats were randomly assigned to receive either sodium selenate (1mg/kg/day), levetiracetam (200/mg/kg/day, a commonly prescribed ASM for TLE) (Mbizvo *et al.*, 2012) or vehicle (saline 0.9%) continuously for 4 weeks. To evaluate the sustained effects of the treatments, video-EEG was acquired before, during, and up to 8 weeks post-treatment, followed by behavioral tests to assess cognitive, and sensorimotor comorbidities. Targeted and untargeted proteomics and metabolomics were performed on brain tissue to investigate potential pathways and molecules associated with modified disease outcomes. Telomere length was investigated as a surrogate marker of disease severity and treatment response. The experimental paradigm is shown in Figure 1 of the Methods section.

Sodium selenate is disease-modifying with enduring effects that reduce the number of seizures in drug-resistant TLE rats.

Video-electroencephalogram (vEEG) was used to examine the effects of the treatments before, during, and up to 8 weeks post-treatment on the occurrence of spontaneous recurrent seizures (Figure 2). Vehicle and levetiracetam-treated animals showed a significant progressive increase in the number of seizures recorded over the course of the experiments [$F(8, 124) = 2.022$, $p < 0.05$]. vEEG analysis during continuous drug treatment (10-14 weeks post-SE) revealed that neither vehicle, sodium selenate, or levetiracetam significantly impacted the number [$F(4, 62) = 0.4781$, $p = 0.751$], duration [$F(2, 43) = 0.5030$, $p = 0.608$], or severity of the seizures [$F(2, 43) = 0.4563$, $p = 0.636$], experienced by post-SE rats, indicating that drug-resistant epilepsy is present 10 weeks after KA-induced SE (Fig 2A). However, following the cessation of treatment, one-way ANOVA showed a treatment effect reducing the number of seizures that the animal experienced [$F(31, 31) = 3.956$, $p < 0.0001$; Fig. 2A]. Tukey's post-hoc analysis

revealed that sodium selenate treatment significantly reduced the number of seizures 8 weeks post-treatment in contrast to vehicle treated animals ($p < 0.05$). Interestingly, four of the twelve sodium selenate treated animals did not manifest any seizures 8 weeks after drug washout, while all of the vehicle and levetiracetam treated animals showed spontaneous seizures through the experiment. In contrast, Tukey's post-hoc showed that levetiracetam treatment did not significantly reduced the number of seizures in comparison to vehicle or selenate treated animals. Average seizure duration [F (1, 15) = 1.038, p = 0.3243; Fig. 2B) and seizure severity, assessed by the Racine scale (Racine, 1972) [F (1, 13) = 0.4873, p = 0.497; Fig. 2C) were not significantly different between the three treatment groups. Figures showing the individual timepoints of the seizure analysis are found in Supplementary Figure S1 A-C.

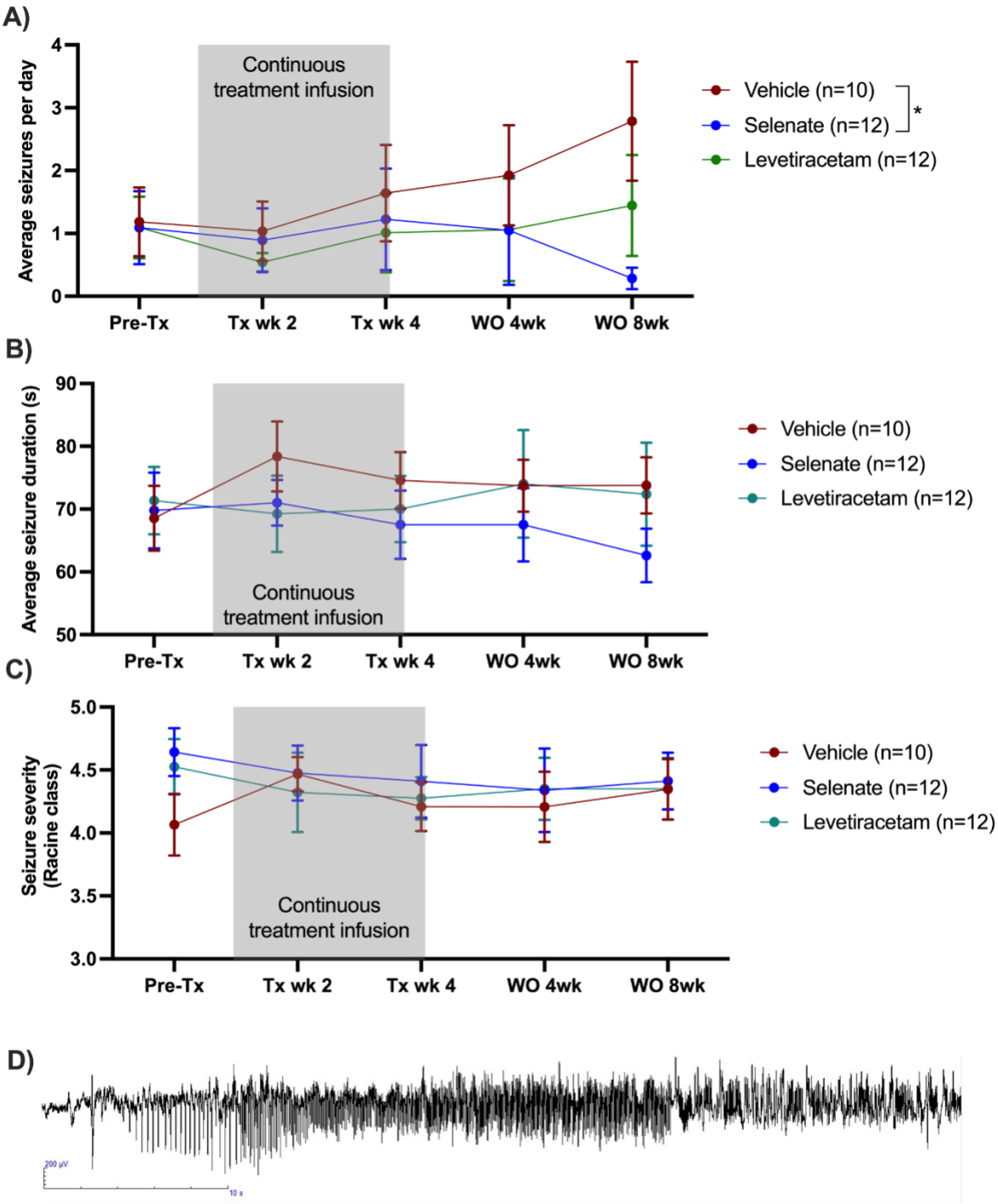

Figure 2: *Sodium selenate has a sustained effect to reduce spontaneous seizures in the post-KA SE rat model of chronic drug-resistant TLE.* **A)** Sodium selenate stopped the progression of seizures from treatment week 4 and significantly reduced seizure frequency 8 weeks after the last day of treatment compared to vehicle treated animals **B)** average seizure duration and **C)** seizure severity were not significantly different between the 3 treatment groups; (*

significantly different from vehicle p <0.05). LEV levetiracetam. Two-way ANOVA with Dunn's *post hoc*. Tx- treatment, wk week, WO, washout. Data shown as mean ± S.E.M. **D)** Representative EEG example of an animal presenting a spontaneous seizure.

Sodium selenate treatment improves spatial memory and recognition memory

Cognitive deficits are one of the most debilitating comorbidities seen in patients with TLE (Hermann *et al.*, 2008; Hermann *et al.*, 2000; Kwan *et al.*, 2011; Sharma *et al.*, 2007; Tellez Zenteno *et al.*, 2007). The novel object placement (NOP) evaluates spatial memory (Spanswick and Sutherland, 2010). Vehicle treated animals had impaired spatial memory in comparison to shams, as they spent significantly less time in the novel location of the object (p <0.05, Fig. 3A). Levetiracetam treatment did not improve spatial memory compared to vehicle. Animals that had been treated with sodium selenate, even after an 8-week washout, spent significantly more time evaluating the novel location of the object than those treated with the vehicle, which is indicative of improved spatial memory (p <0.05). The novel object recognition (NOR) evaluates recognition memory (Spanswick and Sutherland, 2010). Both vehicle and levetiracetam treated rats spent less time evaluating the novel object relative to sham rats (p <0.05, Fig. 3B), which is indicative of impaired recognition memory. In contrast, sodium selenate treatment was also able to improve recognition memory in comparison to vehicle treated rats (p <0.05). Interestingly, the performance of the sodium selenate treated animals was comparable to shams in both the NOP and NOR. Figures showing the individual timepoints of the MWM are found in Supplementary Figure S2 A-B.

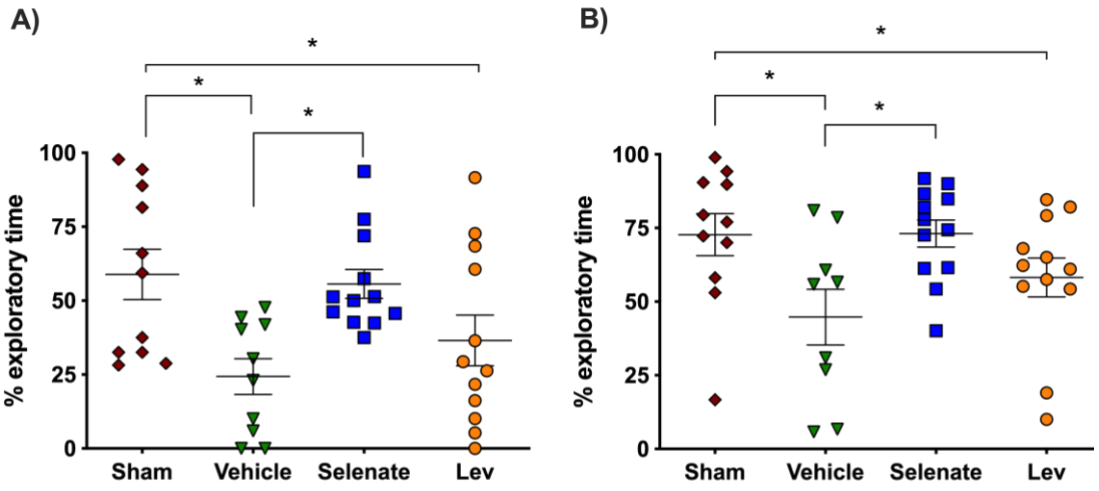

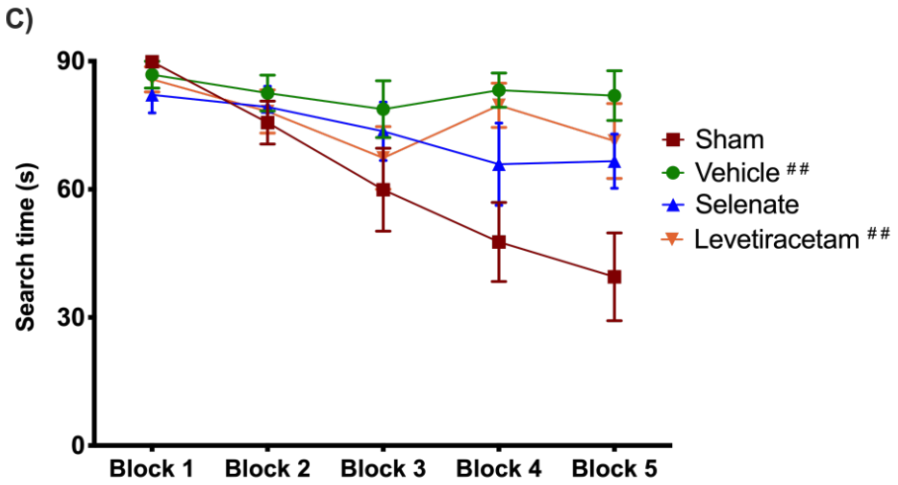

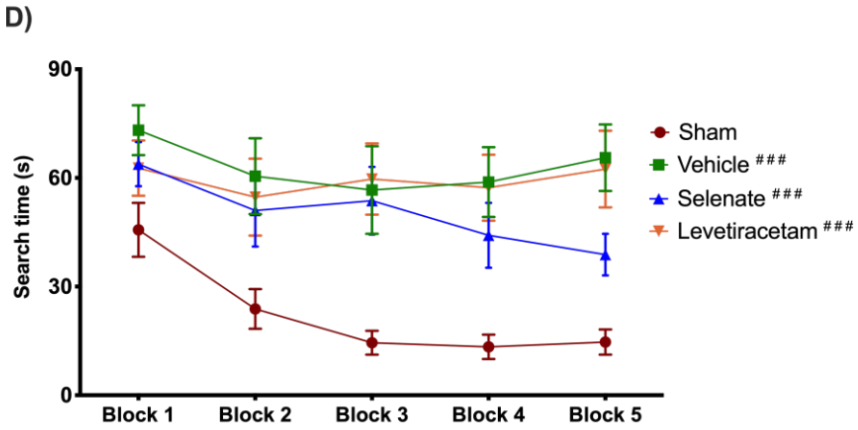

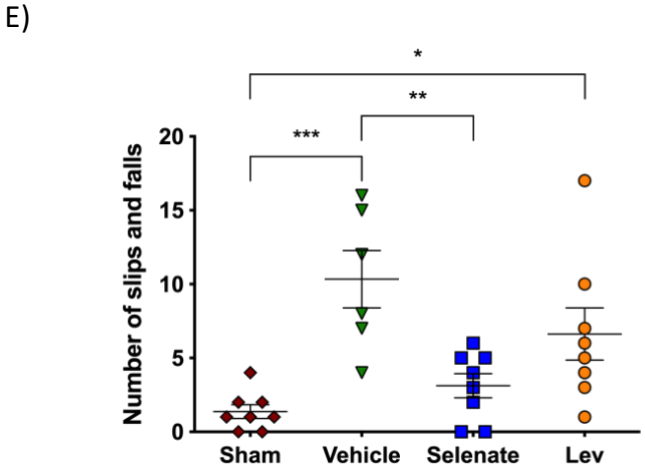

Figure 3: *Sodium selenate improves cognitive and sensorimotor impairments in in the post-KA SE rat model of chronic drug-resistant TLE.* **A)** Novel object placement (NOP). Vehicle and levetiracetam treated animals showed a significantly reduced time examining the novel location of the object compared to shams. In contrast, sodium selenate treatment improved spatial memory in comparison to vehicle in post-SE rats. **B)** Novel object recognition (NOR). Post-SE animals treated with vehicle or levetiracetam showed significantly impaired recognition memory to shams. Sodium selenate rats spent more time evaluating the novel object introduced into the arena in contrast to vehicle, which is a measure of improved recognition memory. **C)** Post-SE rats treated with vehicle and levetiracetam had significantly longer search time in the water maze acquisition session in contrast to shams. D) Water maze reversal, all of the post-SE rats showed significantly longer search times in comparison to sham. For presentation purposes, data for water maze search time is graphed in blocks of two trials. **E)** Post-SE rats treated with vehicle and levetiracetam exhibited more slips and falls on the beast compared to shams. In contrast, treatment with sodium selenate significantly reduced these impairments compared to vehicle. (* p <0.05, ** p <0.01, *** p <0.001; ##p <0.05 and ###p <0.001 significantly different to shams). Kruskal-Wallis with Dunn's post hoc for the NOP and NOR. MWM two-way repeated measures ANOVA, with Dunnett's post hoc. One-way ANOVA with Tukey's post hoc for the beam task. Data shown as mean ± S.E.M.

To further evaluate cognitive function, rats were tested in the Morris water maze (MWM) (Morris, 1984). During the acquisition session of the MWM, only the post-SE rats treated with vehicle and levetiracetam displayed significantly increased search times than their sham counterparts [subject x treatment effects: $F(12, 164) = 2.501$, p <0.01; selenate animals p >0.05 Figure 3C]. One day after the water maze acquisition session, rats underwent a MWM reversal session where the location of the escape platform was changed. Here, all of the post-SE rats cohorts took more time to find the hidden platform in comparison to shams [$F(4, 157) = 5.971$

p <0.001 Figure 3D]. No differences in swim speed were observed between the different groups.

Sodium selenate treatment improves balance in drug-resistant TLE rats.

Rats were tested on the beam task to assess balance and coordination as a measure of sensorimotor function, which is commonly affected in people with drug-resistant TLE (Carter *et al.*, 1999; Carter *et al.*, 2001; Liu *et al.*, 2016). Post-SE rats treated with sodium selenate displayed improved sensorimotor function compared to vehicle as indicated by significantly fewer slips and falls (p <0.01, Fig. 3E). In contrast both vehicle and levetiracetam treated animals showed significantly more slips and falls compared to shams (p <0.001 and p <0.05, respectively). The time to traverse the beam was not significantly different between the groups. No significant findings were observed in either the open field or elevated plus maze tests of anxiety-like behavior. The results of the sucrose preference test are shown in Supplementary Figure S3.

The protein phosphatase family is differentially expressed after treatment with sodium selenate

Sodium selenate has been described to activate PP2A subunit B and to reduce h-tau after traumatic brain injury and in different models of epilepsy (Liu *et al.*, 2016; Shultz *et al.*, 2015). However, to further understand the mechanism by which sodium selenate exerts its disease-modifying effects in our model of established chronic TLE, we utilized state-of-the-art, high-resolution data-independent acquisition mass-spectrometry (DIA-MS), untargeted proteomics and metabolomics analyzes were carried out in the somatosensory cortex and hippocampus to identify potential markers of TLE and on the proteome and metabolome. A total of 5615 and 5538 proteins have been identified and quantified across all samples in the somatosensory cortex and hippocampus, respectively, considering a false discovery rate (q-value) cut-off of 1%. Differential expression analyses using ANOVA revealed 24 proteins in the somatosensory

cortex and 9 proteins in the hippocampus to be significantly dysregulated across all experimental conditions (Figure S4, Supplementary Table S1 and S2). Notably, protein phosphatase 2 regulatory subunit B alpha (Ppp2r5a), heat shock protein family A member 2 (Hspa2) and lymphocyte cytosolic protein 1 (Lcp1) were differentially expressed between selenate and vehicle treated post-SE groups in the somatosensory cortex (Tukey's HSD, *FDR*<0.05, Figure S4A, Supplementary Table S1). Heat shock protein family B member 1 (Hspb1), Ro690 Y RNA binding protein (Ro60) and DENN domain containing 11 (Dennd11) proteins were differentially expressed between selenate and vehicle treated groups in the hippocampus (Tukey's HSD, FDR<0.05, Figure S4B, Supplementary Table S2). To further examine the changes in the proteomic profile of selenate treated rats we performed quantitative gene set enrichment analysis between all pairs of treatment groups. Supplementary Figure S5 shows the top 25 differentially regulated pathways in somatosensory cortex (Supplementary Figure S5A) and hippocampus (Supplementary Figure S5B). Interestingly in the somatosensory cortex of selenate group, amongst the most significantly upregulated pathways were signaling cascades mediated by activated insulin-like growth factor receptors (IGFR) and fibroblast growth factor receptors (FGRF) such as the FGFR-mediated phosphatidylinositol 3-kinase (PI-3K) cascade activation and IGFR1 signaling cascades (*FDR*<0.05). Among the top downregulated pathways in the somatosensory cortex were beta oxidation of fatty acids and iron uptake and transport.

In addition to proteomic analyses, we also performed untargeted univariate metabolomic analyses on the same samples. However, we were not able to identify significant changes between the experimental groups in the somatosensory cortex, suggesting that selenate primarily induces proteomic alterations in this region whilst keeping the metabolome stable (Supplementary Table S3). In contrast six metabolites were significantly different in selenate treated animals as shown in Supplementary Table S4.

Sodium selenate treatment persistently reduces h-tau and increases PP2A protein expression

To further validate the modification of the h-tau pathway by sodium selenate in established TLE, we performed targeted protein analysis of h-tau and PP2A in the somatosensory cortex only due to tissue availability. Semi-automated western blots showed that sodium selenate treatment persistently reduced h-tau compared to vehicle and levetiracetam treated animals (p <0.01 for both comparisons, Supplementary Figure S6A). Similarly, PP2A protein expression was significantly increased in selenate treated animals compared to vehicle (p <0.01), levetiracetam (p <0.01) and shams (p <0.05, Supplementary Figure S6B). No significant differences were found in total tau protein expression.

Sodium selenate treatment reverses telomere shortening in chronic epileptic rats.

Telomere length was investigated as a surrogate marker of epilepsy severity and response to pharmacological treatment (Chan *et al.*, 2020; Galletly *et al.*, 2017; Kang *et al.*, 2020; Lukens *et al.*, 2009). Ear biopsies were taken 25 weeks post-SE to evaluate the effects of chronic epilepsy on telomere length. We found that TLE resulted in telomere shortening in vehicle treated rats (p <0.001), and this was not prevented by levetiracetam treatment (p <0.01). However, sodium selenate treatment was able to reverse telomere shortening seen in post-SE animals treated with vehicle (p <0.01), with the treated rats having telomere length similar to sham animals (Fig. 4).

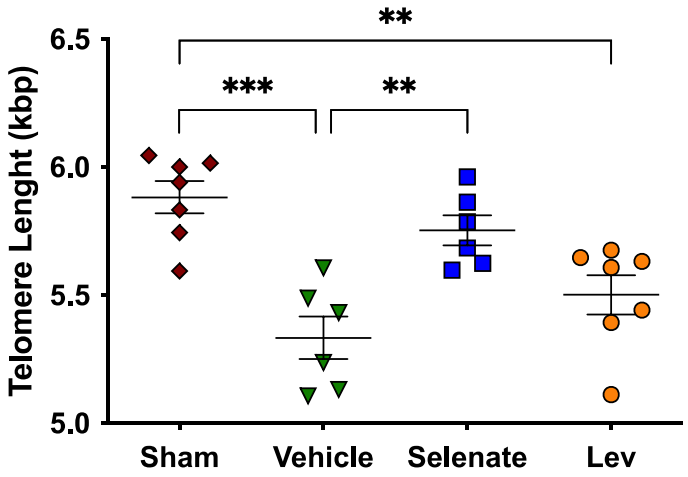

Figure 4: *Sodium selenate prevents telomere shortening in drug-resistant TLE rats.* Chronic post-SE rats treated with levetiracetam and vehicle showed significantly reduced telomere length in comparison to sham. In contrast, sodium selenate treated animals had significantly longer telomeres in comparison to vehicle. kbp, kilobase pairs (* p <0.05, ** p <0.01). One-way ANOVA with Tukey's post hoc. Data shown as mean ± S.E.M.

Seizure burden is correlated with shorter telomeres and poorer cognitive and sensorimotor outcomes.

We also investigated the relationship between the seizure burden (i.e., number of seizures per day) at the end of the 8-week post-treatment washout period, with the different outcomes of the behavioral tests and TL. We found that the number of seizures was inversely correlated with the preference for the novel object in the NOR (r = -0.497, p < 0.001), NOP (r = -0.357, p = 0.016), and TL (r = -0.554, p = 0.005). The number of seizures was correlated with the search time in the MWM (r = 0.436, p = 0.003) and the number of slips and falls in the beam task (r = 0.762, p = 0.001).

Network medicine integration highlights discrete protein-metabolite modules correlate with treatment and pre-clinical outcomes.

Network medicine integration was performed to investigate pathways correlated with the TLE phenotype. We integrated the untargeted multi-omics (proteomics and metabolomics) datasets

with the targeted proteomics and phosphoproteomics (PP2A, tau and h-tau), TLE phenotype (seizures, cognitive and sensorimotor outcomes) and telomere length studies to investigate protein-metabolite groups/pathways correlated with the response to selenate treatment. Weighted correlation network analysis identified 20 and 17 protein-metabolite modules, respectively, in the hippocampal and cortical multi-omic datasets. Several protein-metabolite modules showed significant positive and negative correlations with multiple treatment groups and various clinical measures (Fig. 5A). In the hippocampal network, the Red module is enriched for proteins and metabolites involved in the TCA cycle, oxidative phosphorylation and other metabolic pathways. It is significantly (p = 0.005) inversely correlated with both selenate and levetiracetam treatment groups but has no significant correlation with the vehicle treated post-SE group. The Purple module is also significantly inversely correlated with selenate treatment, and this is enriched for proteins and metabolites involved in aminoacyl-tRNA biosynthesis (*FDR*=0.0059) and Lysine degradation (*FDR*=0.021) pathways. This module is also inversely correlated with levetiracetam treated group has no correlation with the vehicle group. Lastly, the Yellow module is significantly (p =0.007) correlated with the selenate treated group and has no significant correlations with other groups. This module is enriched for proteins and metabolites involved in oxidative phosphorylation and other metabolic pathways.

In the somatosensory cortex correlation network, the Tan (p =0.002), Magenta (p =0.002), Yellow (p =0.02) and Light-cyan (p =0.02) modules were significantly correlated with the selenate treated group and showed no correlation with the vehicle treated group (Fig. 5B). The magenta module does not annotate to any significant pathways; however, the Yellow module is enriched for proteins and metabolites involved in oxidative phosphorylation and other metabolic pathways, and the Tan module annotates to insulin signaling pathway. Lastly,

proteins and metabolites in the Light-cyan module are enriched for fatty acid biosynthesis pathways.

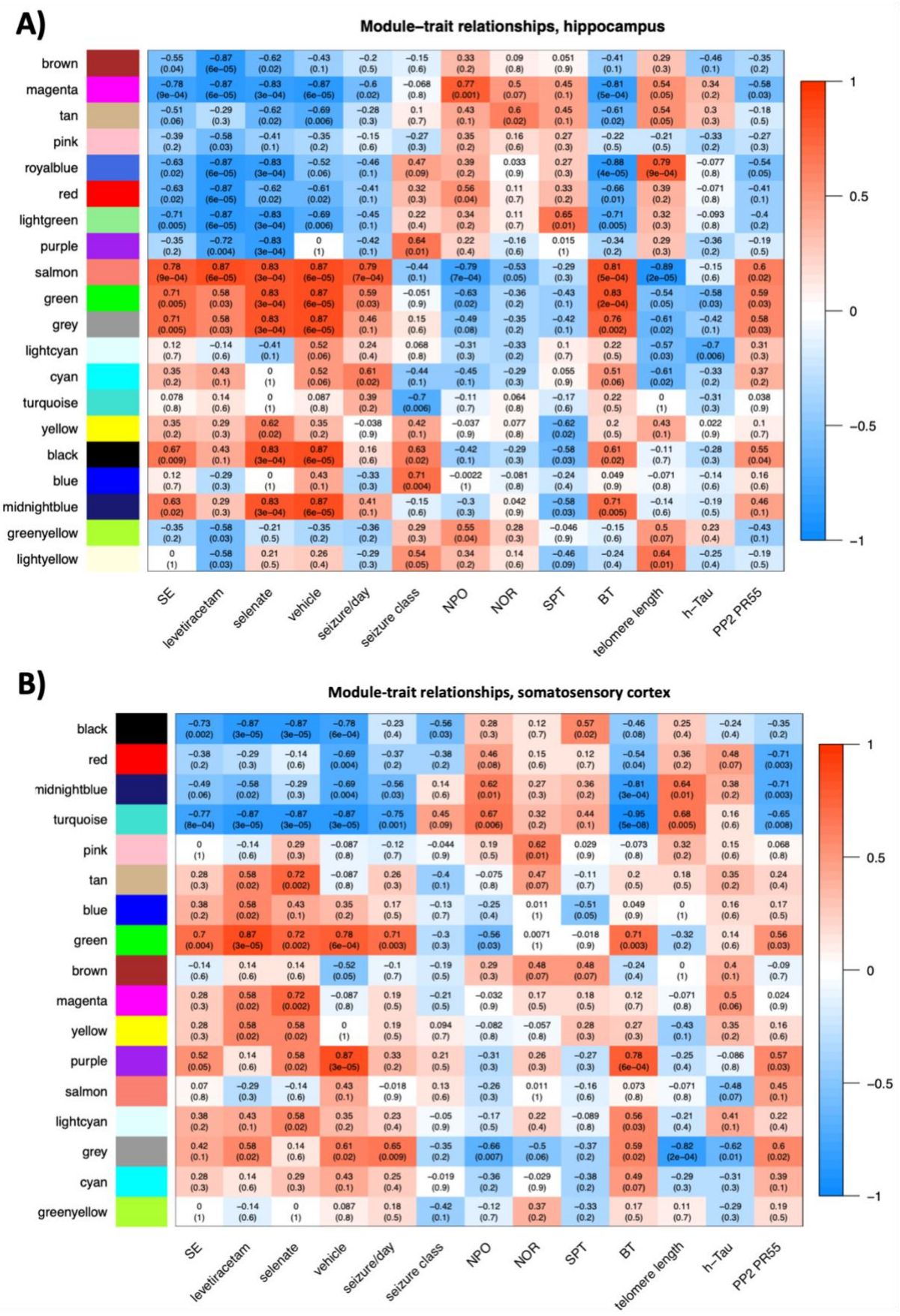

Figure 5. *Somatosensory cortex and hippocampal correlation networks*. The relationship of

protein-metabolite modules (in the Y axis) with measured clinical traits (X axis) in **A)** the hippocampus and **B)** somatosensory cortex. Each square block shows the Spearman correlation coefficient (SCC) of each module with the clinical traits as well as the associated P value in brackets. The SCC values range from -1 to 1, depending on the strength and direction of the correlation.

Discussion

Current medical treatments for TLE, ASMs, are merely symptomatic, attenuating seizures temporarily without any sustained disease-modifying effects on the propensity to have seizures, or its disabling associated neuropsychiatric, cognitive, and sensorimotor comorbidities (Brooks Kayal *et al.*, 2013; Pitkanen *et al.*, 2013; Saletti *et al.*, 2019). Once these treatments are discontinued (or the patient misses a dose), the seizures relapse at least the same severity and frequency as pre-treatment (Coan and Cendes, 2013; Kwan *et al.*, 2011). Here we report for the first time a medical treatment that has persistent disease-modifying effects in an animal model of chronic drug-resistant TLE. Sodium selenate treatment in animals with established epilepsy (i.e., 10 weeks post-KA SE), had an enduring effect mitigating the established epileptic state, and reducing the frequency of seizures and cognitive comorbidities. Our group has previously shown that treatment with sodium selenate in epilepsy models reduces h-tau, increases PP2A, and mitigates the development of epilepsy when delivered immediately after an epileptogenic brain injury, but before the occurrence of spontaneous recurrent seizures (Jones *et al.*, 2012; Liu *et al.*, 2016). However, the most common clinical scenario is that patients present to the clinic with established TLE, weeks to years after the epileptogenic brain insult, and in many patients, there is no identifiable brain insult(Foster *et al.*, 2019).

The data from this study demonstrates that sodium selenate treatment has an enduring effect to mitigate the chronic epileptic state, reducing the frequency of seizures, neurocognitive, sensorimotor and neurobehavioral comorbidities, and biomarkers of disease severity. Strikingly, four of 12 animals (33%), did not have any seizures at all at this timepoint. In contrast, all of the levetiracetam and vehicle treated animals showed spontaneous seizures at the end of the study. Our data supports the proposition that the underlying disease mechanisms associated with chronic TLE may have been modified by the four-week selenate treatment. It is important to note that, analogous to human chronic TLE, spontaneous remission of seizures

is not part of the natural history of the post-KA SE rat model of chronic TLE (Van Nieuwenhuyse *et al.*, 2015a; Williams *et al.*, 2009).

Behavioral comorbidities are considered an integral part of the TLE disease(Brooks Kayal *et al.*, 2013; Mazarati *et al.*, 2018). Patients with chronic and drug-resistant TLE have an increased prevalence of psychiatric conditions, memory and learning disabilities (Kandratavicius *et al.*, 2012; Ott *et al.*, 2003; Stafstrom *et al.*, 1993; Stores, 1971; Tellez Zenteno *et al.*, 2007). Cognitive impairment is the most common comorbidity that afflicts people with TLE and tends to be resistant to treatment, even after epilepsy surgery (Hermann *et al.*, 2000). In fact, in a proportion of cases, the cognitive dysfunction progresses despite successful seizure control (Amlerova *et al.*, 2014; Berg *et al.*, 2012; Smith *et al.*, 2014; Taylor *et al.*, 2010). In keeping with the human condition, cognitive deficits have been demonstrated as a comorbidity in the post-SE animal model (Detour *et al.*, 2005; Pearson *et al.*, 2014) (Chauvière *et al.*, 2009). Here we found that animals treated with sodium selenate had improved spatial memory and recognition memory, comparable to non-epileptic controls. This is the first time that a treatment has been described to reverse memory deficits in established chronic TLE.

Sensorimotor deficits are another significant comorbidity in people with TLE (Girardi-Schappo *et al.*, 2021) (Gandelman-Marton *et al.*, 2006), and are not necessarily associated with the presence of seizures or with the use of ASMs (Gandelman-Marton *et al.*, 2006; Petty *et al.*, 2010; Shiek Ahmad *et al.*, 2015). A study in patients with drug-resistant TLE found abnormal postural instability and increased risk of falls than healthy controls (Gandelman-Marton *et al.*, 2006). Interestingly, transgenic mouse models that expressed h-tau have been described to not only present cognitive dysfunction but also sensorimotor impairments (Kreilaus *et al.*, 2021; Leroy *et al.*, 2007; Lewis *et al.*, 2000). Here, we found that sodium selenate treatment mitigated

the sensorimotor deficits in chronically epileptic rats in the post-KA SE model of TLE.

The results from this study add to the growing literature that indicate that pathological h-tau is a key pathophysiological driver of drug-resistant TLE and associated comorbidities. To further test this hypothesis, we performed untargeted proteomics using DIA-MS and targeted h-tau and PP2A protein analysis using Western Blots. Our data suggests that the persistent disease-modifying effects of sodium selenate in drug-resistant TLE may be exerted via its effects on increasing the expression of the B catalytic subunit of PP2A and the consequent reduction of h-tau. Evidence has shown that PP2A B subunit is specifically involved in the dephosphorylation of tau (Barnes *et al.*, 1995; Corcoran *et al.*, 2010a) and PP2A expression and activity are potentiated by sodium selenate (Corcoran *et al.*, 2010a; Jones *et al.*, 2012; Shultz *et al.*, 2015).

In accordance with animal models(Corcoran *et al.*, 2010b; Jones *et al.*, 2012; Shultz *et al.*, 2015), increased levels and deposits of h-tau have been described in surgically resected tissue from patients with drug-resistant TLE (Puvenna *et al.*, 2016; Sanchez *et al.*, 2018; Sen *et al.*, 2007; Tai *et al.*, 2016; Thom *et al.*, 2011). In resected tissue from patients with drug-resistant TLE, PP2A protein expression is also significantly decreased, but remains unchanged in Alzheimer's disease patients, indicating that PP2A alterations may be an epilepsy-specific pathology (Gourmaud *et al.*, 2020). There is also building evidence that tau-based mechanisms enhance neuronal excitability. Alterations in tau phosphorylation have been implicated in changing the excitation/inhibition balance in the neurons (Palop *et al.*, 2007). Unstable microtubule assembly at axonal segments, as seen with the presence of h-tau, dysregulate the resting membrane potential and thereby generations of action potentials (Matsumoto and Sakai, 1979). Tau is transported into cell via Fyn kinase where it influences N-methyl-D-aspartate (NMDA) receptor mediated excitotoxicity (van Eersel *et al.*, 2010) and changes in tau has been

correlated with dysfunction of axonal NMDA receptors which are all considered mechanisms that promote the expression of seizures (Liu *et al.*, 2017).

Pathological h-tau, has been proposed as one of the main culprits underlying cognitive deficits across different neurodegenerative disorders such as Alzheimer's disease, TBI, and epilepsy (Casillas-Espinosa, 2020). Accumulation of h-tau in temporal lobe brain tissue from patients with drug-resistant TLE is associated with cognitive decline (Gourmaud *et al.*, 2020; Thom *et al.*, 2011). Furthermore, tau pathology has been associated with a decline in verbal learning, recall and graded naming test scores in different neurodegenerative disorders(Tai *et al.*, 2016) and in animal models that overexpressed h-tau (Kreilaus *et al.*, 2021; Leroy *et al.*, 2007; Lewis *et al.*, 2000).

It is interesting that for some of the animals the effects of sodium selenate were only observed several weeks after cessation of treatment, and the magnitude of the decrease in seizure expression progressively increased over the 8 weeks of follow-up post-treatment. One possibility could be that the processes required to mitigate epileptic activity in neurons takes time, particularly in chronically epileptic animals. However, it is also possible that the effects of sodium selenate extend beyond the described modification of h-tau and PP2A.

Dimension reduction is crucial for hypothesis generation to elucidate pathological mechanisms and changes in biological pathways as a response to treatment. To further understand sodium selenate's mechanism of action, we performed a network medicine integration of our untargeted/targeted multi-omics datasets, TLE outcomes (seizures and behavior) and TLE studies to evaluate the correlation coefficients of single modules between the different treatment groups (e.g., Selenate and Vehicle). By mapping significant genes/proteins together with metabolites to biological pathways, our network integration approach allowed for

reduction in experimental and biological noise and higher confidence levels, thereby generating potential new disease modules (proteins and metabolites and the cellular pathways they are involved in). We found modules that constitute the "healthy state", which operate in a concerted fashion in a healthy brain but are lost in the setting of TLE. The *Green Module* is positively correlated to epilepsy phenotype, poor cognitive performance, poor balance, shorter telomeres, decreased PP2A, increased h-tau expression, and cardiomyopathies, which have been shown to be associated with several epilepsy syndromes (Devinsky *et al.*, 2018; Gilchrist, 1963; Naggar *et al.*, 2014; Stöllberger *et al.*, 2011; Surges and Sander, 2012). Of particular interest are the *Yellow-Module* in both the hippocampal and somatosensory cortex correlation networks as well as *Tan* and *Light-cyan Modules* in the somatosensory cortex. All of the above-mentioned modules positively correlated with selenate treatment. The *Yellow Module* is enriched for pathways involved in ATP metabolism, oxidative phosphorylation, and several inflammatory systems. The *Tan Module* is enriched for insulin signaling pathways and the *Light-cyan Module* annotates to fatty acid metabolism pathways. It is important to note that "enrichment" does not mean "increase" or "upregulation". The enrichment in insulin signaling, for example, highlights the involvement of this pathway in the epilepsy phenotype and selenate treatment, but unfortunately provides no information about the direction of change (upregulation or downregulation). In an attempt to capture changes in regulation of biological pathways that may be influenced by sodium selenate treatment we conducted a quantitative enrichment analysis on a pathway level (PADOG) between the selenate and vehicle groups, utilizing the Reactome pathway database resource. Based on the PADOG analysis results, there is significant upregulation of IGFR1 and FGFR signaling cascades and FGFR-mediated PI-3K cascade activation in the selenate treated group compared to vehicle. Given the neuroprotective role of PI-3K signaling in several epilepsy syndromes, it is conceivable that this is one of the potential mechanisms by which sodium selenate exerts its long-term disease

modifying effect. The strong correlation of the *Tan Module*, which annotates to insulin signaling pathways to selenate treatment only further highlights the involvement of insulin signaling in the potential mechanism of action of this treatment. The downregulation of fatty acid oxidation processes in the selenate group suggests a shift from hyperactive neurons with high-energy demand (like in epileptic seizures) towards neurons with lower energy demand.

Further investigation of these pathways as potential mechanisms involved in the mode of action of sodium selenate can be instrumental in understanding and reversing the drug-resistance of TLE. To our knowledge, this analysis is the first attempt of integration of metabolomic and proteomic data in an epilepsy network medicine paradigm. We demonstrate that multi-omic, data-driven correlation networks can be used for agnostic, hypothesis-free examination of disease states as well as identification of specific protein-metabolite modules associated with different states and treatments.

Prognostic biomarkers are used to predict disease characteristics and identify disease recurrence or progression in patients who have the disease of interest. Unfortunately, no such prognostic biomarkers for TLE currently exist (Simonato *et al.*, 2021). Telomere length has emerged as a potential prognostic biomarker of chronic neurodegenerative conditions (Chan *et al.*, 2020; Kang *et al.*, 2020) (Galletly *et al.*, 2017; Lukens *et al.*, 2009). Telomeres are repetitive non-coding DNA-tandem sequences of TTAGGG found at the end of eukaryotic chromosomes (Hehar and Mychasiuk, 2016). Telomere length has been used as a biological marker for cellular aging and has been described in many neurological disorders (Hehar and Mychasiuk, 2016; Koppelstaetter *et al.*, 2009; Sun *et al.*, 2019; Wright *et al.*, 2018), including TLE (Miranda *et al.*, 2020). Here we analyzed telomere length from ear biopsies, as previous evidence has shown strong correlation between telomere length in brain and peripheral skin cells(Hehar and Mychasiuk, 2016). We found that telomere length was significantly reduced

in TLE animals treated with vehicle or levetiracetam, and that treatment with sodium selenate reduced telomere length shortening. The magnitude of the reduced telomere length was strongly associated with the number of seizures and more pronounced cognitive deficits in our drug-resistant TLE model. Overall, our data highlights the potential of telomere length as a prognostic biomarker of disease severity, treatment response, and TLE disease modification, that has potential to be used in further trials of DMT.

Conclusion

This study reports novel data that demonstrates that modulating h-tau by sodium selenate treatment for 4 weeks has disease modifying effects in an animal model of chronic drug-resistant TLE. Even though, different pre-clinical treatments, including sodium selenate, have previously been described to have anti-epileptogenic effects immediately after the epileptogenic brain injury in animal models (Casillas-Espinosa *et al.*, 2019b; Liu *et al.*, 2016; Zhong Huang *et al.*, 2019), this is the first time a medical treatment has been shown to have disease modifying properties in chronically epileptic animals. This approach is highly translatable, given that sodium selenate has already been shown to be safe and well tolerated in early phase clinical trials for other conditions (Cardoso *et al.*, 2019; Corcoran *et al.*, 2010b; Malpas *et al.*, 2016; Vivash *et al.*, 2020), and there are a large number of patients with chronic drug resistant TLE. The findings of this study, if confirmed in clinical trials, could be paradigm shifting for the treatment of this common and highly disabling disease.

Acknowledgements

This study used BPA-enabled (Bioplatforms Australia) / NCRIS-enabled (National Collaborative Research Infrastructure Strategy) infrastructure located at the Monash Proteomics & Metabolomics Facility led by RBS.

PMCE was funded by a NHMRC Early Career Fellowship (#APP1087172) and the University of Melbourne Early Career Research Grant (#603834). RM – Canadian Institutes for Health Research (CIHR) PTJ – 153051. SRS is supported by a NHMRC Level 2 Career Development Fellowship.

Competing interests

The authors report no competing interests related to the current work.

1

References

Alonso-Vanegas, M.A., Cisneros-Franco, J.M., Castillo-Montoya, C., Martínez-Rosas, A.R., Gómez-Pérez, M.E., Rubio-Donnadieu, F., 2013. Self-reported quality of life in pharmacoresistant temporal lobe epilepsy: correlation with clinical variables and memory evaluation. *Epileptic Disord.* 15**,** 263-271.

Amlerova, J., Cavanna, A.E., Bradac, O., Javurkova, A., Raudenska, J., Marusic, P., 2014. Emotion recognition and social cognition in temporal lobe epilepsy and the effect of epilepsy surgery. *Epilepsy Behav.* 36**,** 86-89.

Bao, F., Shultz, S.R., Hepburn, J.D., Omana, V., Weaver, L.C., Cain, D.P., Brown, A., 2012. A CD11d monoclonal antibody treatment reduces tissue injury and improves neurological outcome after fluid percussion brain injury in rats. *J. Neurotrauma* 29**,** 2375-2392.

Barker-Haliski, M.L., Friedman, D., French, J.A., White, H.S., 2015. Disease modification in epilepsy: from animal models to clinical applications. *Drugs* 75**,** 749-767.

Barnes, G.N., Slevin, J.T., Vanaman, T.C., 1995. Rat brain protein phosphatase 2A: an enzyme that may regulate autophosphorylated protein kinases. *J. Neurochem.* 64**,** 340-353.

Berg, A.T., Zelko, F.A., Levy, S.R., Testa, F.M., 2012. Age at onset of epilepsy, pharmacoresistance, and cognitive outcomes: a prospective cohort study. *Neurology* 79**,** 1384-1391.

Bhandare, A.M., Kapoor, K., Powell, K.L., Braine, E., Casillas-Espinosa, P., O'Brien, T.J., Farnham, M.M.J., Pilowsky, P.M., 2017. Inhibition of microglial activation with minocycline at the intrathecal level attenuates sympathoexcitatory and proarrhythmogenic changes in rats with chronic temporal lobe epilepsy. *Neuroscience* 350**,** 23-38.

Brady, R., Wong, K., Robinson, D., Mychasiuk, R., McDonald, S., D'Cunha, R., Yamakawa, G., Sun, M., Wark, J., Lee, P.V.S., O'Brien, T., Casillas Espinosa, P., Shultz, S., 2019. Bone Health in Rats With Temporal Lobe Epilepsy in the Absence of Anti-Epileptic Drugs. *Front. Pharmacol.* 10**,** 1278-1278.

Brandt, C., Glien, M., Gastens, A.M., Fedrowitz, M., Bethmann, K., Volk, H.A., Potschka, H., Loscher, W., 2007. Prophylactic treatment with levetiracetam after status epilepticus: lack of effect on epileptogenesis, neuronal damage, and behavioral alterations in rats. *Neuropharmacology* 53**,** 207-221.

Broadbent, N.J., Squire, L.R., Clark, R.E., 2004. Spatial memory, recognition memory, and the hippocampus. *Proc. Natl. Acad. Sci. U. S. A.* 101**,** 14515-14520.

Brooks Kayal, A., Bath, K., Berg, A., Galanopoulou, A., Holmes, G., Jensen, F., Kanner, A., O'Brien, T., Whittemore, V., Winawer, M., Patel, M., Scharfman, H., 2013. Issues related to symptomatic and disease-modifying treatments affecting cognitive and neuropsychiatric comorbidities of epilepsy. *Epilepsia* 54 Suppl 4**,** 44-60.

Cardoso, B.R., Roberts, B.R., Malpas, C.B., Vivash, L., Genc, S., Saling, M.M., Desmond, P., Steward, C., Hicks, R.J., Callahan, J., Brodtmann, A., Collins, S., Macfarlane, S., Corcoran, N.M., Hovens, C.M., Velakoulis, D., O'Brien, T.J., Hare, D.J., Bush, A.I., 2019. Supranutritional Sodium Selenate Supplementation Delivers Selenium to the Central Nervous System: Results from a Randomized Controlled Pilot Trial in Alzheimer's Disease. *Neurotherapeutics* 16**,** 192-202.

Carter, R.J., Lione, L.A., Humby, T., Mangiarini, L., Mahal, A., Bates, G.P., Dunnett, S.B., Morton, A.J., 1999. Characterization of progressive motor deficits in mice transgenic for the human Huntington's disease mutation. *J. Neurosci.* 19**,** 3248-3257.

Carter, R.J., Morton, J., Dunnett, S.B., 2001. Motor coordination and balance in rodents. *Curr. Protoc. Neurosci.* Chapter 8**,** Unit 8.12.

Casillas Espinosa, P., Andrade, P., Santana Gomez, C., Ali, I., Brady, R., Smith, G., Immonen, R., Puhakka, N., Hudson, M., Pitkänen, A., Shultz, S., Jones, N., Staba, R., O'Brien, T., 2019. Harmonization of the pipeline for seizure detection to phenotype post-traumatic epilepsy in a preclinical multicenter study on post-traumatic epileptogenesis.

Casillas Espinosa, P., Hicks, A., Jeffreys, A., Snutch, T., O'Brien, T., Powell, K., 2015. Z944, a Novel Selective T-Type Calcium Channel Antagonist Delays the Progression of Seizures in the Amygdala Kindling Model. *PLoS One* 10**,** e0130012.

Casillas-Espinosa, P.M., Sargsyan, A., Melkonian, D., O'Brien, T.J., 2019a. A universal automated tool for reliable detection of seizures in rodent models of acquired and genetic epilepsy. *Epilepsia* 60**,** 783-791.

Casillas-Espinosa, P.M., Shultz, S.R., Braine, E.L., Jones, N.C., Snutch, T.P., Powell, K.L., O'Brien, T.J., 2019b. Disease-modifying effects of a novel T-type calcium channel antagonist, Z944, in a model of temporal lobe epilepsy. *Prog. Neurobiol.*, 101677.

Casillas-Espinosa, P.M.A., I.; O'Brien, T.J., 2020. Neurodegenerative pathways as targets for acquired epilepsy therapy development. *Epilepsia Open* 10.

Cawthon, R.M., 2002. Telomere measurement by quantitative PCR. *Nucleic Acids Res.* 30, e47.

Chan, D., Martin-Ruiz, C., Saretzki, G., Neely, D., Qiu, W., Kunadian, V., 2020. The association of telomere length and telomerase activity with adverse outcomes in older patients with non-ST-elevation acute coronary syndrome. *PLoS One* 15, e0227616.

Chauvière, L., Rafrafi, N., Thinus-Blanc, C., Bartolomei, F., Esclapez, M., Bernard, C., 2009. Early deficits in spatial memory and theta rhythm in experimental temporal lobe epilepsy. *The Journal of neuroscience : the official journal of the Society for Neuroscience* 29, 5402-5410.

Chen, Z., Brodie, M.J., Liew, D., Kwan, P., 2018. Treatment Outcomes in Patients With Newly Diagnosed Epilepsy Treated With Established and New Antiepileptic Drugs: A 30-Year Longitudinal Cohort Study. *JAMA Neurol* 75, 279-286.

Coan, A.C., Cendes, F., 2013. Epilepsy as progressive disorders: what is the evidence that can guide our clinical decisions and how can neuroimaging help? *Epilepsy Behav.* 26, 313-321.

Corcoran, N., Martin, D., Hutter Paier, B., Windisch, M., Nguyen, T., Nheu, L., Sundstrom, L., Costello, A., Hovens, C., 2010a. Sodium selenate specifically activates PP2A phosphatase, dephosphorylates tau and reverses memory deficits in an Alzheimer's disease model. *J. Clin. Neurosci.* 17, 1025-1033.

Corcoran, N.M., Hovens, C.M., Michael, M., Rosenthal, M.A., Costello, A.J., 2010b. Open-label, phase I dose-escalation study of sodium selenate, a novel activator of PP2A, in patients with castration-resistant prostate cancer. *Br. J. Cancer* 103, 462-468.

Creek, D.J., Anderson, J., McConville, M.J., Barrett, M.P., 2012. Metabolomic analysis of trypanosomatid protozoa. *Mol Biochem Parasitol* 181, 73-84.

Detour, J., Schroeder, H., Desor, D., Nehlig, A., 2005. A 5-month period of epilepsy impairs spatial memory, decreases anxiety, but spares object recognition in the lithium-pilocarpine model in adult rats. *Epilepsia* 46, 499-508.

Devinsky, O., Kim, A., Friedman, D., Bedigian, A., Moffatt, E., Tseng, Z.H., 2018. Incidence of cardiac fibrosis in SUDEP and control cases. *Neurology* 91, e55-e61.

Dezsi, G., Ozturk, E., Stanic, D., Powell, K.L., Blumenfeld, H., O'Brien, T.J., Jones, N.C., 2013. Ethosuximide reduces epileptogenesis and behavioral comorbidity in the GAERS model of genetic generalized epilepsy. *Epilepsia* 54, 635-643.

Fabregat, A., Jupe, S., Matthews, L., Sidiropoulos, K., Gillespie, M., Garapati, P., Haw, R., Jassal, B., Korninger, F., May, B., Milacic, M., Roca, C.D., Rothfels, K., Sevilla, C., Shamovsky, V., Shorser, S., Varusai, T., Viteri, G., Weiser, J., Wu, G., Stein, L., Hermjakob, H., D'Eustachio, P., 2018. The Reactome Pathway Knowledgebase. *Nucleic Acids Res* 46, D649-D655.

Foster, E., Carney, P., Liew, D., Ademi, Z., O'Brien, T., Kwan, P., 2019. First seizure presentations in adults: beyond assessment and treatment. *Journal of neurology, neurosurgery, and psychiatry* 90, 1039-1045.

Galletly, C., Dhillon, V.S., Liu, D., Balzan, R.P., Hahn, L.A., Fenech, M.F., 2017. Shorter telomere length in people with schizophrenia: A preliminary study from Australia. *Schizophr. Res.* 190, 46-51.

Gandelman-Marton, R., Arlazoroff, A., Dvir, Z., 2006. Balance performance in adult epilepsy patients. *Seizure* 15, 582-589.

Gilchrist, L., 1963. CARDIOMYOPATHY, TEMPORAL LOBE EPILEPSY AND PREGNANCY. *Proc. R. Soc. Med.* 56, 923.

Girardi-Schappo, M., Fadaie, F., Lee, H.M., Caldairou, B., Sziklas, V., Crane, J., Bernhardt, B.C., Bernasconi, A., Bernasconi, N., 2021. Altered communication dynamics reflect cognitive deficits in temporal lobe epilepsy. *Epilepsia* 62, 1022-1033.

Gourmaud, S., Shou, H., Irwin, D.J., Sansalone, K., Jacobs, L.M., Lucas, T.H., Marsh, E.D., Davis, K.A., Jensen, F.E., Talos, D.M., 2020. Alzheimer-like amyloid and tau alterations associated with cognitive deficit in temporal lobe epilepsy. *Brain* 143, 191-209.

Hehar, H., Mychasiuk, R., 2016. The use of telomere length as a predictive biomarker for injury prognosis in juvenile rats following a concussion/mild traumatic brain injury. *Neurobiol. Dis.* 87, 11-18.

Hermann, B., Seidenberg, M., Jones, J., 2008. The neurobehavioural comorbidities of epilepsy: can a natural history be developed? *Lancet Neurol.* 7, 151-160.

Hermann, B.P., Seidenberg, M., Bell, B., Woodard, A., Rutecki, P., Sheth, R., 2000. Comorbid psychiatric symptoms in temporal lobe epilepsy: association with chronicity of epilepsy and impact on quality of life. *Epilepsy Behav.* 1**,** 184-190.

Hinnell, C., Williams, J., Metcalfe, A., Patten, S.B., Parker, R., Wiebe, S., Jette, N., 2010. Health status and health-related behaviors in epilepsy compared to other chronic conditions--a national population-based study. *Epilepsia* 51**,** 853-861.

Ittner, L., Götz, J., 2011. Amyloid-β and tau--a toxic pas de deux in Alzheimer's disease. *Nature Reviews. Neuroscience* 12**,** 65-72.

Janssens, V., Goris, J., 2001. Protein phosphatase 2A: a highly regulated family of serine/threonine phosphatases implicated in cell growth and signalling. *Biochem. J.* 353**,** 417-439.

Jassal, B., Matthews, L., Viteri, G., Gong, C., Lorente, P., Fabregat, A., Sidiropoulos, K., Cook, J., Gillespie, M., Haw, R., Loney, F., May, B., Milacic, M., Rothfels, K., Sevilla, C., Shamovsky, V., Shorser, S., Varusai, T., Weiser, J., Wu, G., Stein, L., Hermjakob, H., D'Eustachio, P., 2020. The reactome pathway knowledgebase. *Nucleic Acids Res* 48**,** D498-D503.

Johnstone, V.P., Wright, D.K., Wong, K., O'Brien, T.J., Rajan, R., Shultz, S.R., 2015. Experimental Traumatic Brain Injury Results in Long-Term Recovery of Functional Responsiveness in Sensory Cortex but Persisting Structural Changes and Sensorimotor, Cognitive, and Emotional Deficits. *J. Neurotrauma* 32**,** 1333-1346.

Jones, N., Nguyen, T., Corcoran, N., Velakoulis, D., Chen, T., Grundy, R., O'Brien, T., Hovens, C., 2012. Targeting hyperphosphorylated tau with sodium selenate suppresses seizures in rodent models. *Neurobiol. Dis.* 45**,** 897-901.

Jones, N.C., Salzberg, M.R., Kumar, G., Couper, A., Morris, M.J., O'Brien, T.J., 2008. Elevated anxiety and depressive-like behavior in a rat model of genetic generalized epilepsy suggesting common causation. *Exp. Neurol.* 209**,** 254-260.

Kandratavicius, L., Lopes Aguiar, C., Bueno Júnior, L., Romcy Pereira, R., Hallak, J.E.C., Leite, J., 2012. Psychiatric comorbidities in temporal lobe epilepsy: possible relationships between psychotic disorders and involvement of limbic circuits. *Revista Brasileira de Psiquiatria* 34**,** 454-466.

Kang, J.I., Mueller, S.G., Wu, G.W.Y., Lin, J., Ng, P., Yehuda, R., Flory, J.D., Abu-Amara, D., Reus, V.I., Gautam, A., Hammamieh, R., Doyle, F.J., 3rd, Jett, M., Marmar, C.R., Mellon, S.H., Wolkowitz, O.M., 2020. Effect of Combat Exposure and Posttraumatic Stress Disorder on Telomere Length and Amygdala Volume. *Biol Psychiatry Cogn Neurosci Neuroimaging* 5**,** 678-687.

Kolb, B., Whishaw, I.Q., 1985. Earlier is not always better: behavioral dysfunction and abnormal cerebral morphogenesis following neonatal cortical lesions in the rat. *Behav. Brain Res.* 17**,** 25-43.

Koppelstaetter, C., Kern, G., Mayer, G., 2009. Biomarkers of aging with prognostic and predictive value in non-oncological diseases. *Curr. Med. Chem.* 16**,** 3469-3475.

Kreilaus, F., Masanetz, R., Watt, G., Przybyla, M., Ittner, A., Ittner, L., Karl, T., 2021. The behavioural phenotype of 14-month-old female TAU58/2 transgenic mice. *Behav Brain Res* 397**,** 112943.

Kwan, P., Schachter, S.C., Brodie, M.J., 2011. Drug-resistant epilepsy. *N. Engl. J. Med.* 365**,** 919-926.

Langfelder, P., Horvath, S., 2008. WGCNA: an R package for weighted correlation network analysis. *BMC Bioinformatics* 9**,** 559.

Leroy, K., Bretteville, A., Schindowski, K., Gilissen, E., Authelet, M., De Decker, R., Yilmaz, Z., Buée, L., Brion, J.P., 2007. Early axonopathy preceding neurofibrillary tangles in mutant tau transgenic mice. *Am. J. Pathol.* 171**,** 976-992.

Lewis, J., McGowan, E., Rockwood, J., Melrose, H., Nacharaju, P., Van Slegtenhorst, M., Gwinn-Hardy, K., Paul Murphy, M., Baker, M., Yu, X., Duff, K., Hardy, J., Corral, A., Lin, W.L., Yen, S.H., Dickson, D.W., Davies, P., Hutton, M., 2000. Neurofibrillary tangles, amyotrophy and progressive motor disturbance in mice expressing mutant (P301L) tau protein. *Nat. Genet.* 25**,** 402-405.

Li, C., Silva, J., Ozturk, E., Dezsi, G., O'Brien, T.J., Renoir, T., Jones, N.C., 2018. Chronic fluoxetine treatment accelerates kindling epileptogenesis in mice independently of 5-HT2A receptors. 59**,** e114-e119.

Liu, S.J., Zheng, P., Wright, D.K., Dezsi, G., Braine, E., Nguyen, T., Corcoran, N.M., Johnston, L.A., Hovens, C.M., Mayo, J.N., Hudson, M., Shultz, S.R., Jones, N.C., O'Brien, T.J., 2016. Sodium selenate retards epileptogenesis in acquired epilepsy models reversing changes in protein phosphatase 2A and hyperphosphorylated tau. *Brain* 139**,** 1919-1938.

Liu, X., Ou, S., Yin, M., Xu, T., Wang, T., Liu, Y., Ding, X., Yu, X., Yuan, J., Huang, H., Zhang, X., Tan, X., Chen, L., Chen, Y., 2017. N-methyl-D-aspartate receptors mediate epilepsy-induced axonal impairment and tau phosphorylation via activating glycogen synthase kinase-3β and cyclin-dependent kinase 5. *Discov. Med.* 23**,** 221-234.

Loscher, W., Honack, D., 1993. Profile of ucb L059, a novel anticonvulsant drug, in models of partial and generalized epilepsy in mice and rats. *Eur. J. Pharmacol.* 232**,** 147-158.

Loscher, W., Honack, D., Rundfeldt, C., 1998. Antiepileptogenic effects of the novel anticonvulsant levetiracetam (ucb L059) in the kindling model of temporal lobe epilepsy. *J Pharmacol Exp Ther* 284**,** 474-479.

Lukens, J.N., Van Deerlin, V., Clark, C.M., Xie, S.X., Johnson, F.B., 2009. Comparisons of telomere lengths in peripheral blood and cerebellum in Alzheimer's disease. *Alzheimers Dement* 5**,** 463-469.

Malpas, C., Vivash, L., Genc, S., Saling, M., Desmond, P., Steward, C., Hicks, R., Callahan, J., Brodtmann, A., Collins, S., Macfarlane, S., Corcoran, N., Hovens, C., Velakoulis, D., O'Brien, T., 2016. A Phase IIa Randomized Control Trial of VEL015 (Sodium Selenate) in Mild-Moderate Alzheimer's Disease. *Journal of Alzheimer's disease* 54**,** 223-232.

Matsumoto, G., Sakai, H., 1979. Microtubules inside the plasma membrane of squid giant axons and their possible physiological function. *J. Membr. Biol.* 50**,** 1-14.

Mazarati, A., Jones, N.C., Galanopoulou, A.S., Harte-Hargrove, L.C., Kalynchuk, L.E., Lenck-Santini, P.P., Medel-Matus, J.S., Nehlig, A., de la Prida, L.M., Sarkisova, K., Veliskova, J., 2018. A companion to the preclinical common data elements on neurobehavioral comorbidities of epilepsy: a report of the TASK3 behavior working group of the ILAE/AES Joint Translational Task Force. *Epilepsia Open* 3**,** 24-52.

Mbizvo, G.K., Dixon, P., Hutton, J.L., Marson, A.G., 2012. Levetiracetam add-on for drug-resistant focal epilepsy: an updated Cochrane Review. *Cochrane Database Syst. Rev.* 2012**,** Cd001901.

Miranda, D.M., Rosa, D.V., Costa, B.S., Nicolau, N.F., Magno, L.A.V., de Paula, J.J., Romano-Silva, M.A., 2020. Telomere shortening in patients with drug-resistant epilepsy. *Epilepsy Res.* 166**,** 106427.

Morris, R., 1984. Developments of a water-maze procedure for studying spatial learning in the rat. *J. Neurosci. Methods* 11**,** 47-60.

Morris, R.G., 1989. Synaptic plasticity and learning: selective impairment of learning rats and blockade of long-term potentiation in vivo by the N-methyl-D-aspartate receptor antagonist AP5. *The Journal of neuroscience* 9**,** 3040-3057.

Naggar, I., Lazar, J., Kamran, H., Orman, R., Stewart, M., 2014. Relation of autonomic and cardiac abnormalities to ventricular fibrillation in a rat model of epilepsy. *Epilepsy Res.* 108**,** 44-56.

Ndode Ekane, X., Santana Gomez, C., Casillas Espinosa, P., Ali, I., Brady, R., Smith, G., Andrade, P., Immonen, R., Puhakka, N., Hudson, M., Braine, E., Shultz, S., Staba, R., O'Brien, T., Pitkänen, A., 2019. Harmonization of lateral fluid-percussion injury model production and post-injury monitoring in a preclinical multicenter biomarker discovery study on post-traumatic epileptogenesis. *Epilepsy Res.* 151**,** 7-16.

O'Brien, T.J., Ben-Menachem, E., Bertram, E.H., 3rd, Collins, S.D., Kokaia, M., Lerche, H., Klitgaard, H., Staley, K.J., Vaudano, E., Walker, M.C., Simonato, M., 2013. Proposal for a "phase II" multicenter trial model for preclinical new antiepilepsy therapy development. *Epilepsia* 54 Suppl 4**,** 70-74.

Ott, D., Siddarth, P., Gurbani, S., Koh, S., Tournay, A., Shields, W.D., Caplan, R., 2003. Behavioral disorders in pediatric epilepsy: unmet psychiatric need. *Epilepsia* 44**,** 591-597.

Palop, J.J., Chin, J., Roberson, E.D., Wang, J., Thwin, M.T., Bien-Ly, N., Yoo, J., Ho, K.O., Yu, G.Q., Kreitzer, A., Finkbeiner, S., Noebels, J.L., Mucke, L., 2007. Aberrant excitatory neuronal activity and compensatory remodeling of inhibitory hippocampal circuits in mouse models of Alzheimer's disease. *Neuron* 55**,** 697-711.

Pang, Z., Chong, J., Zhou, G., de Lima Morais, D.A., Chang, L., Barrette, M., Gauthier, C., Jacques, P., Li, S., Xia, J., 2021. MetaboAnalyst 5.0: narrowing the gap between raw spectra and functional insights. *Nucleic Acids Res.* 49**,** W388-w396.

Pauletti, A., Terrone, G., Shekh-Ahmad, T., Salamone, A., Ravizza, T., Rizzi, M., Pastore, A., Pascente, R., Liang, L.P., Villa, B.R., Balosso, S., Abramov, A.Y., van Vliet, E.A., Del Giudice, E., Aronica, E., Patel, M., Walker, M.C., Vezzani, A., 2019. Targeting oxidative stress improves disease outcomes in a rat model of acquired epilepsy. *Brain* 142**,** e39.

Paxinos, G., Watson, C., 1982. *The rat brain in stereotaxic coordinates*. Academic Press: Sydney.

Pearson, J.N., Schulz, K.M., Patel, M., 2014. Specific alterations in the performance of learning and memory tasks in models of chemoconvulsant-induced status epilepticus. *Epilepsy Res.* 108**,** 1032-1040.

Perucca, P., Gilliam, F.G., 2012. Adverse effects of antiepileptic drugs. *Lancet Neurol.* 11**,** 792-802.

Petty, S.J., Hill, K.D., Haber, N.E., Paton, L.M., Lawrence, K.M., Berkovic, S.F., Seibel, M.J., O'Brien, T.J., Wark, J.D., 2010. Balance impairment in chronic antiepileptic drug users: a twin and sibling study. *Epilepsia* 51**,** 280-288.

Pitkanen, A., Kharatishvili, I., Narkilahti, S., Lukasiuk, K., Nissinen, J., 2005. Administration of diazepam during status epilepticus reduces development and severity of epilepsy in rat. *Epilepsy Res.* 63**,** 27-42.

Pitkanen, A., Nehlig, A., Brooks-Kayal, A.R., Dudek, F.E., Friedman, D., Galanopoulou, A.S., Jensen, F.E., Kaminski, R.M., Kapur, J., Klitgaard, H., Loscher, W., Mody, I., Schmidt, D., 2013. Issues related to development of antiepileptogenic therapies. *Epilepsia* 54**,** 35-43.

Puvenna, V., Engeler, M., Banjara, M., Brennan, C., Schreiber, P., Dadas, A., Bahrami, A., Solanki, J., Bandyopadhyay, A., Morris, J.K., Bernick, C., Ghosh, C., Rapp, E., Bazarian, J.J., Janigro, D., 2016. Is phosphorylated tau unique to chronic traumatic encephalopathy? Phosphorylated tau in epileptic brain and chronic traumatic encephalopathy. *Brain Res.* 1630**,** 225-240.

Racine, R.J., 1972. Modification of seizure activity by electrical stimulation. II. Motor seizure. *Electroencephalogr. Clin. Neurophysiol.* 32**,** 281-294.

Rizzi, M., Brandt, C., Weissberg, I., Milikovsky, D.Z., Pauletti, A., Terrone, G., Salamone, A., Frigerio, F., Loscher, W., Friedman, A., Vezzani, A., 2019. Changes of dimension of EEG/ECoG nonlinear dynamics predict epileptogenesis and therapy outcomes. *Neurobiol. Dis.* 124**,** 373-378.

Saletti, P.G., Ali, I., Casillas-Espinosa, P.M., Semple, B.D., Lisgaras, C.P., Moshe, S.L., Galanopoulou, A.S., 2019. In search of antiepileptogenic treatments for post-traumatic epilepsy. *Neurobiol. Dis.* 123**,** 86-99.

Sanchez, M.P., Garcia-Cabrero, A.M., Sanchez-Elexpuru, G., Burgos, D.F., Serratosa, J.M., 2018. Tau-Induced Pathology in Epilepsy and Dementia: Notions from Patients and Animal Models. *Int J Mol Sci* 19.

Santana-Gomez, C., Andrade, P., Hudson, M.R., Paananen, T., Ciszek, R., Smith, G., Ali, I., Rundle, B.K., Ndode-Ekane, X.E., Casillas-Espinosa, P.M., Immonen, R., Puhakka, N., Jones, N., Brady, R.D., Perucca, P., Shultz, S.R., Pitkanen, A., O'Brien, T.J., Staba, R., 2019. Harmonization of pipeline for detection of HFOs in a rat model of post-traumatic epilepsy in preclinical multicenter study on post-traumatic epileptogenesis. *Epilepsy Res.***,** 106110.

Sarkisova, K.Y., Midzianovskaia, I.S., Kulikov, M.A., 2003. Depressive-like behavioral alterations and c-fos expression in the dopaminergic brain regions in WAG/Rij rats with genetic absence epilepsy. *Behav. Brain Res.* 144**,** 211-226.

Scheltema, R.A., Jankevics, A., Jansen, R.C., Swertz, M.A., Breitling, R., 2011. PeakML/mzMatch: a file format, Java library, R library, and tool-chain for mass spectrometry data analysis. *Anal. Chem.* 83**,** 2786-2793.

Sen, A., Thom, M., Martinian, L., Harding, B., Cross, J.H., Nikolic, M., Sisodiya, S., 2007. Pathological tau tangles localize to focal cortical dysplasia in older patients. *Epilepsia* 48**,** 1447-1454.

Sharma, A.K., Reams, R.Y., Jordan, W.H., Miller, M.A., Thacker, H.L., Snyder, P.W., 2007. Mesial temporal lobe epilepsy: pathogenesis, induced rodent models and lesions. *Toxicol. Pathol.* 35**,** 984-999.

Shiek Ahmad, B., Wark, J.D., Petty, S.J., O'Brien, T.J., Gorelik, A., Sambrook, P.N., Hill, K.D., 2015. Changes in balance function with chronic antiepileptic drug therapy: A twin and sibling study. *Epilepsia* 56**,** 1714-1722.

Shultz, S.R., Wright, D.K., Zheng, P., Stuchbery, R., Liu, S.J., Sashindranath, M., Medcalf, R.L., Johnston, L.A., Hovens, C.M., Jones, N.C., O'Brien, T.J., 2015. Sodium selenate reduces hyperphosphorylated tau and improves outcomes after traumatic brain injury. *Brain* 138**,** 1297-1313.

Simonato, M., Agoston, D.V., Brooks-Kayal, A., Dulla, C., Fureman, B., Henshall, D.C., Pitkänen, A., Theodore, W.H., Twyman, R.E., Kobeissy, F.H., Wang, K.K., Whittemore, V., Wilcox, K.S., 2021. Identification of clinically relevant biomarkers of epileptogenesis - a strategic roadmap. *Nat. Rev. Neurol.* 17**,** 231-242.

Simonato, M., Brooks-Kayal, A.R., Engel, J., Jr., Galanopoulou, A.S., Jensen, F.E., Moshe, S.L., O'Brien, T.J., Pitkanen, A., Wilcox, K.S., French, J.A., 2014. The challenge and promise of anti-epileptic therapy development in animal models. *Lancet Neurol.* 13**,** 949-960.

Simonato, M., French, J.A., Galanopoulou, A.S., O'Brien, T.J., 2013. Issues for new antiepilepsy drug development. *Curr. Opin. Neurol.* 26**,** 195-200.

Smith, M.L., Olds, J., Snyder, T., Elliott, I., Lach, L., Whiting, S., 2014. A follow-up study of cognitive function in young adults who had resective epilepsy surgery in childhood. *Epilepsy Behav.* 32**,** 79-83.

Spanswick, S.C., Sutherland, R.J., 2010. Object/context-specific memory deficits associated with loss of hippocampal granule cells after adrenalectomy in rats. *Learn. Mem.* 17**,** 241-245.

Srivastava, P.K., Bagnati, M., Delahaye-Duriez, A., Ko, J.H., Rotival, M., Langley, S.R., Shkura, K., Mazzuferi, M., Danis, B., van Eyll, J., Foerch, P., Behmoaras, J., Kaminski, R.M., Petretto, E., Johnson, M.R., 2017. Genome-wide analysis of differential RNA editing in epilepsy. *Genome Res* 27**,** 440-450.

Stafstrom, C.E., Chronopoulos, A., Thurber, S., Thompson, J.L., Holmes, G.L., 1993. Age-dependent cognitive and behavioral deficits after kainic acid seizures. *Epilepsia* 34**,** 420-432.

Stöllberger, C., Wegner, C., Finsterer, J., 2011. Seizure-associated Takotsubo cardiomyopathy. *Epilepsia* 52**,** e160-167.

Stores, G., 1971. Cognitive function in children with epilepsy. *Dev. Med. Child Neurol.* 13**,** 390-393.

Sun, M., Brady, R.D., Casillas-Espinosa, P.M., Wright, D.K., Semple, B.D., Kim, H.A., Mychasiuk, R., Sobey, C.G., O'Brien, T.J., Vinh, A., McDonald, S.J., Shultz, S.R., 2019. Aged rats have an altered immune response and worse outcomes after traumatic brain injury. *Brain. Behav. Immun.* 80**,** 536-550.

Surges, R., Sander, J.W., 2012. Sudden unexpected death in epilepsy: mechanisms, prevalence, and prevention. *Curr Opin Neurol* 25**,** 201-207.

Tai, X., Koepp, M., Duncan, J., Fox, N., Thompson, P., Baxendale, S., Liu, J.Y.W., Reeves, C., Michalak, Z., Thom, M., 2016. Hyperphosphorylated tau in patients with refractory epilepsy correlates with cognitive decline: a study of temporal lobe resections. *Brain* 139**,** 2441-2455.

Tautenhahn, R., Böttcher, C., Neumann, S., 2008. Highly sensitive feature detection for high resolution LC/MS. *BMC Bioinformatics* 9**,** 504.

Taylor, J., Kolamunnage-Dona, R., Marson, A.G., Smith, P.E., Aldenkamp, A.P., Baker, G.A., 2010. Patients with epilepsy: cognitively compromised before the start of antiepileptic drug treatment? *Epilepsia* 51**,** 48-56.

Taylor, R.S., Sander, J.W., Taylor, R.J., Baker, G.A., 2011. Predictors of health-related quality of life and costs in adults with epilepsy: a systematic review. *Epilepsia* 52**,** 2168-2180.

Tellez Zenteno, J., Patten, S., Jetté, N., Williams, J., Wiebe, S., 2007. Psychiatric comorbidity in epilepsy: a population-based analysis. *Epilepsia* 48**,** 2336-2344.

Téllez-Zenteno, J.F., Dhar, R., Wiebe, S., 2005. Long-term seizure outcomes following epilepsy surgery: a systematic review and meta-analysis. *Brain* 128**,** 1188-1198.

Thom, M., Liu, J.Y.W., Thompson, P., Phadke, R., Narkiewicz, M., Martinian, L., Marsdon, D., Koepp, M., Caboclo, L., Catarino, C., Sisodiya, S., 2011. Neurofibrillary tangle pathology and Braak staging in chronic epilepsy in relation to traumatic brain injury and hippocampal sclerosis: a post-mortem study. *Brain* 134**,** 2969-2981.

Thomson, K.E., Metcalf, C.S., Newell, T.G., Huff, J., Edwards, S.F., West, P.J., Wilcox, K.S., 2020. Evaluation of subchronic administration of antiseizure drugs in spontaneously seizing rats. *Epilepsia* 61**,** 1301-1311.

Valente, K.D.R., Busatto Filho, G., 2013. Depression and temporal lobe epilepsy represent an epiphenomenon sharing similar neural networks: clinical and brain structural evidences. *Arq. Neuropsiquiatr.* 71**,** 183-190.

van Eersel, J., Ke, Y., Liu, X., Delerue, F., Kril, J., Götz, J., Ittner, L., 2010. Sodium selenate mitigates tau pathology, neurodegeneration, and functional deficits in Alzheimer's disease models. *Proc. Natl. Acad. Sci. U. S. A.* 107**,** 13888-13893.

Van Nieuwenhuyse, B., Raedt, R., Delbeke, J., Sprengers, M., Dauwe, I., Gadeyne, S., Wadman, W., Boon, P., Vonck, K., 2015a. Hippocampal dbs affects disease development in the ka rat model for tle. *Epilepsy Curr.* 15**,** 577.

Van Nieuwenhuyse, B., Raedt, R., Sprengers, M., Dauwe, I., Gadeyne, S., Carrette, E., Delbeke, J., Wadman, W.J., Boon, P., Vonck, K., 2015b. The systemic kainic acid rat model of temporal lobe epilepsy: Long-term EEG monitoring. *Brain Res.* 1627**,** 1-11.

Vivash, L., Malpas, C.B., Churilov, L., Walterfang, M., Brodtmann, A., Piguet, O., Ahmed, R.M., Bush, A.I., Hovens, C.M., Kalincik, T., Darby, D., Velakoulis, D., O'Brien, T.J., 2020. A study protocol for a phase II randomised, double-blind, placebo-controlled trial of sodium selenate as a disease-modifying treatment for behavioural variant frontotemporal dementia. *BMJ Open* 10**,** e040100.

Whishaw, I.Q., Jarrard, L.E., 1995. Similarities vs. differences in place learning and circadian activity in rats after fimbria-fornix section or ibotenate removal of hippocampal cells. *Hippocampus* 5**,** 595-604.

Williams, P.A., White, A.M., Clark, S., Ferraro, D.J., Swiercz, W., Staley, K.J., Dudek, F.E., 2009. Development of spontaneous recurrent seizures after kainate-induced status epilepticus. *J Neurosci* 29**,** 2103-2112.

Wright, D., O'Brien, T., Mychasiuk, R., Shultz, S., 2018. Telomere length and advanced diffusion MRI as biomarkers for repetitive mild traumatic brain injury in adolescent rats. *NeuroImage: Clinical* 18**,** 315-324.

Zeng, L.-H., Rensing, N., Wong, M., 2009. The mammalian target of rapamycin signaling pathway mediates epileptogenesis in a model of temporal lobe epilepsy. *The Journal of neuroscience* 29**,** 6964-6972.

Zhang, G., He, P., Tan, H., Budhu, A., Gaedcke, J., Ghadimi, B.M., Ried, T., Yfantis, H.G., Lee, D.H., Maitra, A., Hanna, N., Alexander, H.R., Hussain, S.P., 2013. Integration of metabolomics and transcriptomics revealed a fatty acid network exerting growth inhibitory effects in human pancreatic cancer. *Clin Cancer Res* 19**,** 4983-4993.

Zhong Huang, Y., He, X.P., Krishnamurthy, K., McNamara, J.O., 2019. TrkB-Shc signaling protects against hippocampal injury following status epilepticus. *J. Neurosci.* 39**,** 4624-4630.

Supplementary material

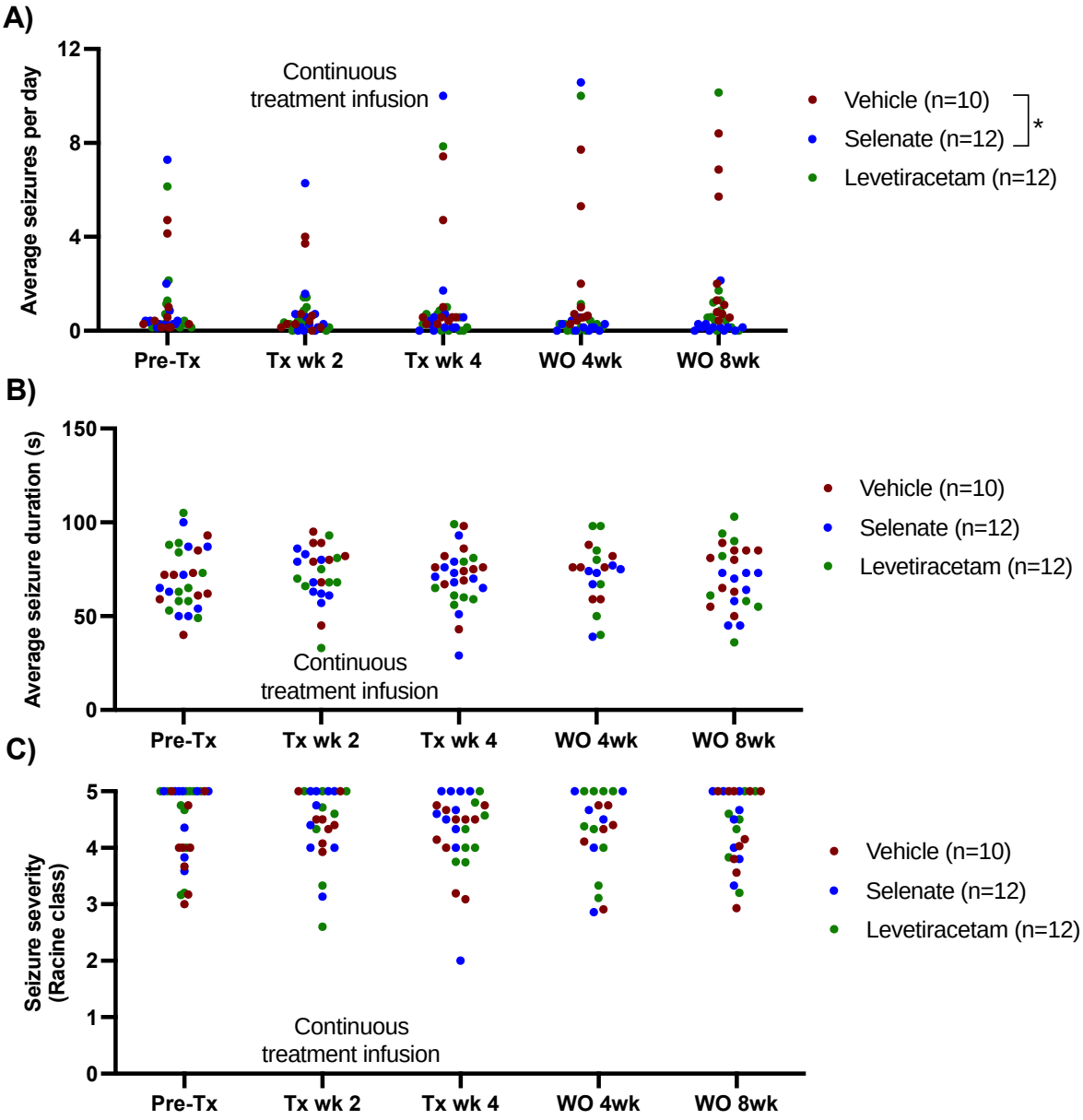

Supplementary Figure S1: *Seizure analysis - Single data points:* **A)** Sodium selenate stopped the progression of seizures from treatment week 4 and significantly reduced seizure frequency 8 weeks after the last day of treatment compared to vehicle treated animals **B)** average seizure duration and **C)** seizure severity were not significantly different between the 3 treatment groups; (* significantly different from vehicle p <0.05). LEV levetiracetam. Two-way ANOVA with Dunn's *post hoc*. Tx- treatment, wk week, WO, washout. Data shown as mean ± S.E.M.

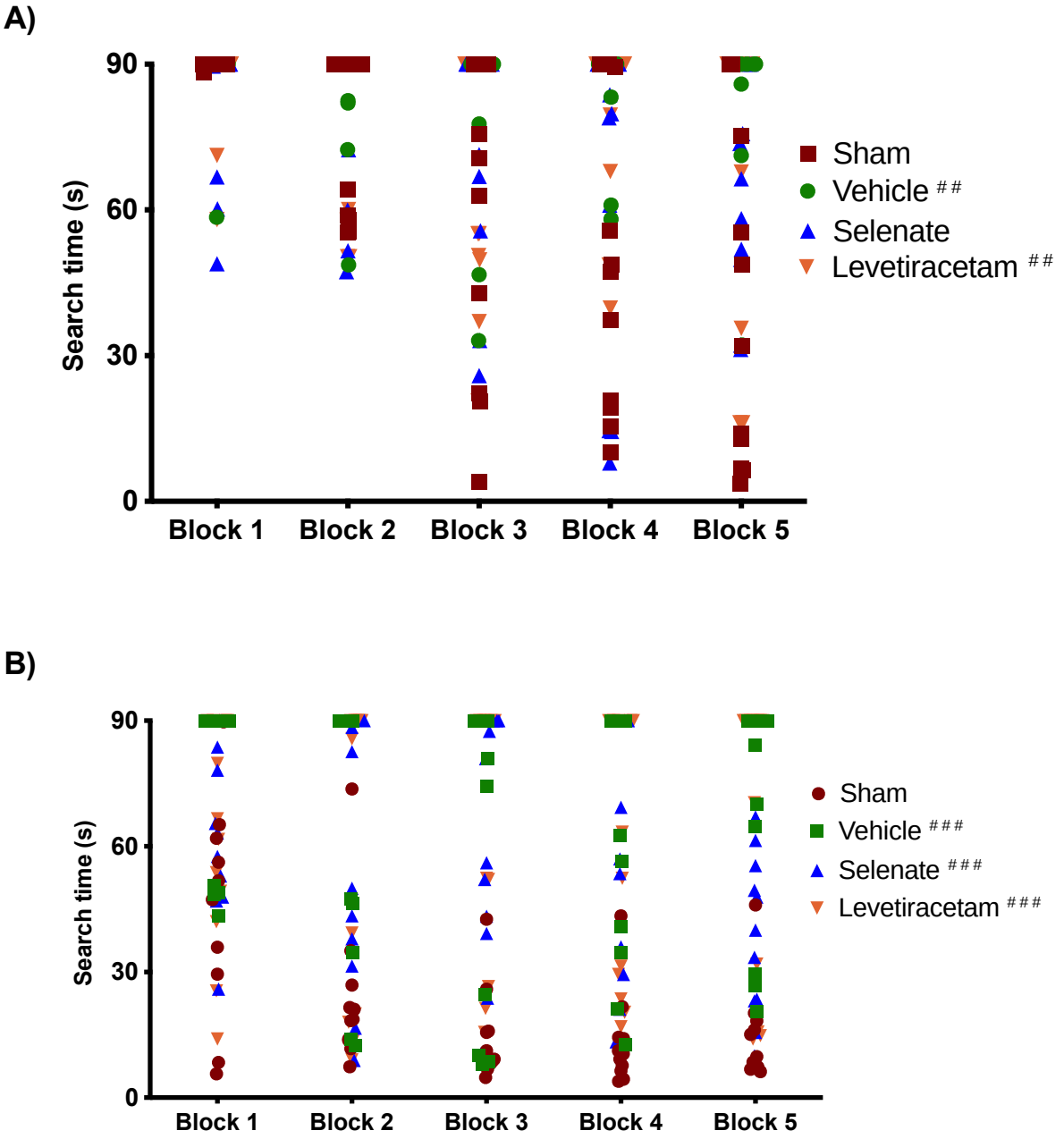

Supplementary Figure S2: *Morris Water Maze - Single data points.* **A)** Post-SE rats treated with vehicle and levetiracetam had significantly longer search time in the water maze acquisition session in contrast to shams. **B)** Water maze reversal, all the post-SE rats showed significantly longer search times in comparison to sham. For presentation purposes, data for water maze search time is graphed in blocks of two trials. (* p <0.05, ** p <0.01, *** p <0.001; ##p <0.05 and ###p <0.001 significantly different to shams). Two-way repeated measures ANOVA, with Dunnett's post hoc. Data shown as mean ± S.E.M.

Post-SE rats develop depressive-like behavior in the sucrose preference test.

Reduced sucrose preference can be interpreted as anhedonia, one of the major diagnostic criteria of depressive-like disorders in humans (Casillas-Espinosa *et al.*, 2019b; Jones *et al.*, 2008). Analysis of the 24-hour SPT showed that post-SE animals treated with vehicle had a reduced preference for the 2% sucrose solution when compared to shams ($P < 0.05$, Supplementary Figure S1). Sucrose preference was not significantly different between selenate, levetiracetam and shams.

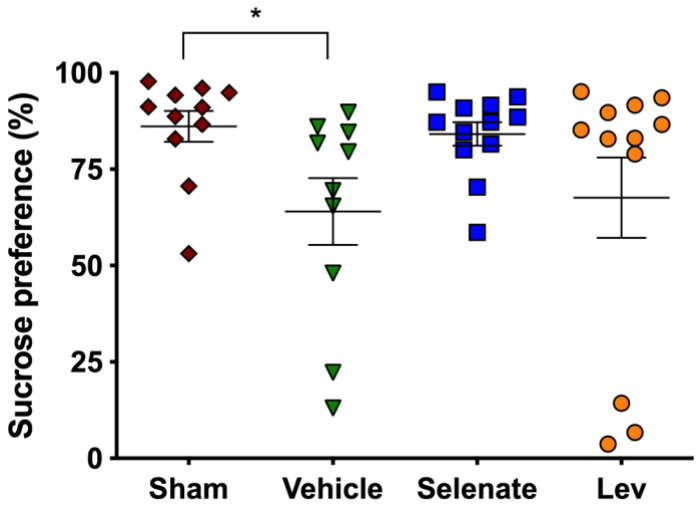

Supplementary Figure S3: *Post-SE rats show depressive-like behavior as assessed by the sucrose preference test.* Post-SE animals treated with vehicle had a reduced sucrose preference compared to shams (* $p < 0.05$). One-way ANOVA with Tukey's post hoc. Data shown as mean ± S.E.M.

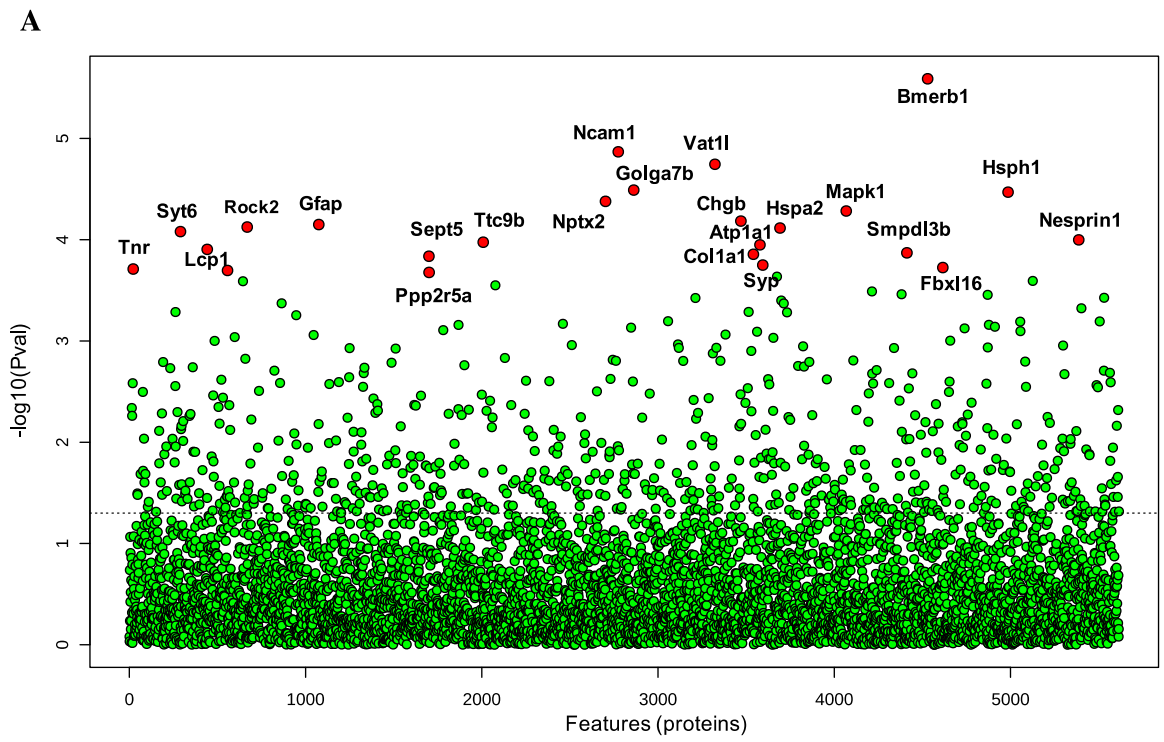

1

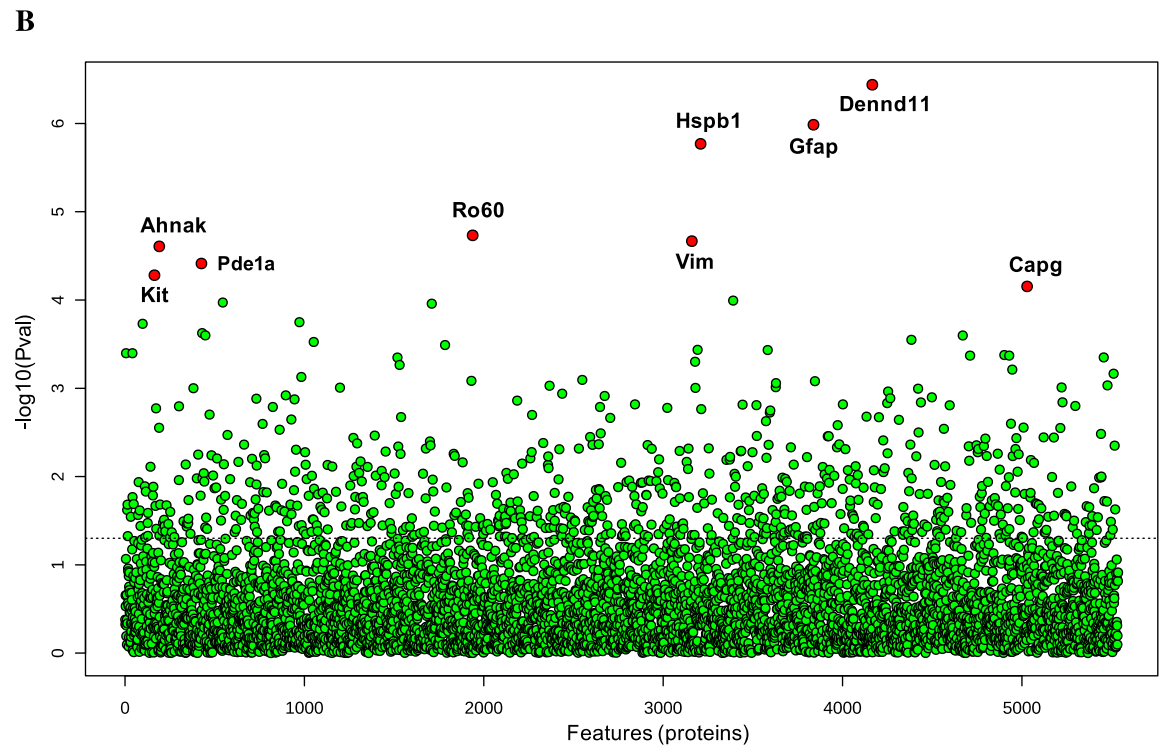

2

3 **Supplementary Figure S4.** *Differential expression analysis of all detected proteins* in **A)** somatosensory cortex
4 and **B)** hippocampus of all post-SE treatment groups and shams. One-way ANOVA was used to identify difference
5 in protein abundance among selenate, levetiracetam and vehicle treated groups and shams. Difference between
6 specific groups was determined via Tukey's honestly significant difference (HSD) test. Significance threshold

1 was set to FDR< 0.05, significantly different proteins are labelled red.

2

A

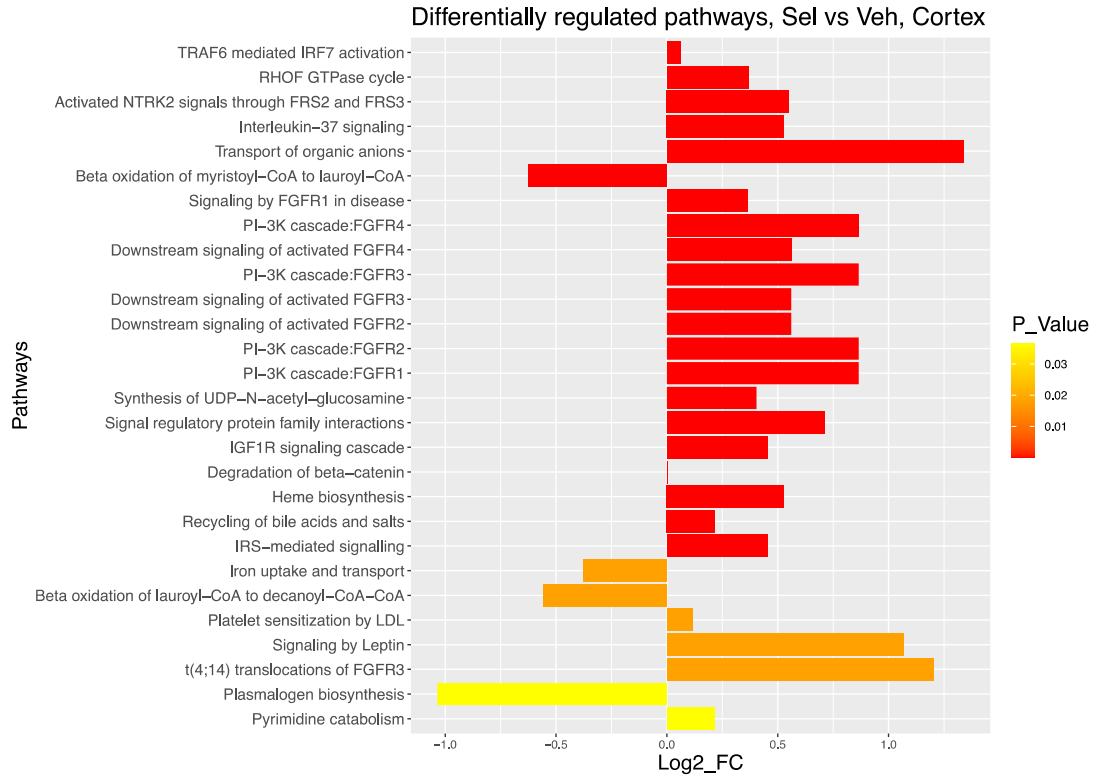

1

B

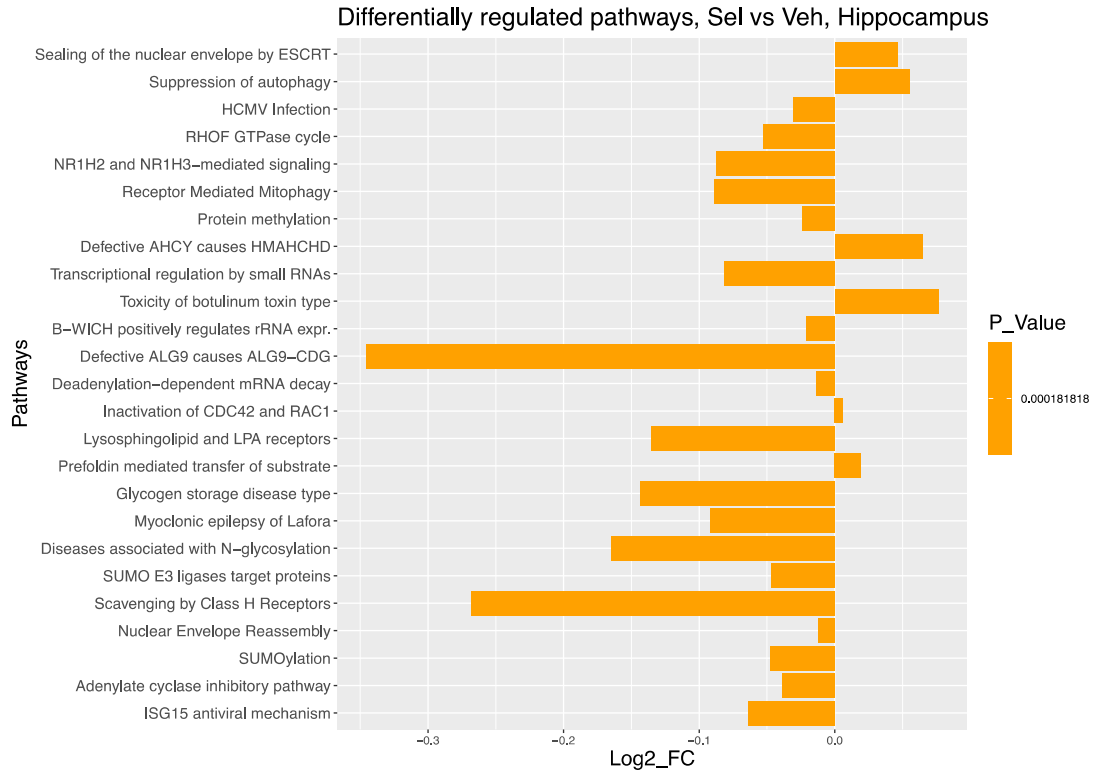

2

Supplementary Figure S5. *The top 25 differentially regulated pathways* in the **A)** somatosensory cortex and **B)** hippocampus of selenate treated rats compared to vehicle group. The quantitative enrichment analysis (PADOG) was carried out using the Reactome database resource. The Log2_FC (X axis) indicates the direction of pathway regulation. Pathways with adjusted P-value of < 0.05 were considered differentially regulated between selenate and vehicle groups. All Reactome pathways were manually curated and organized hierarchically.

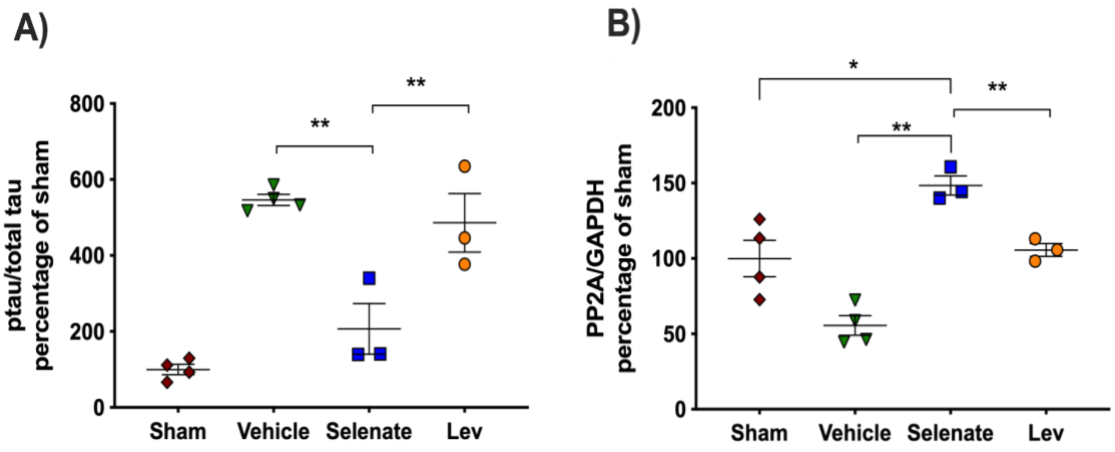

Supplementary Figure S6: *Sodium selenate modifies hyperphosphorylated-tau and PP2A expression.* Post-mortem analysis of brain tissue showed that sodium selenate had persistent effects in reducing hyperphosphorylated-tau in **A)** the somatosensory cortex of drug-resistant TLE rats. Similarly, **B)** PP2A expression was significantly increased in the sodium selenate somatosensory cortex in comparison to the other treatment groups (* $p < 0.05$, ** $P<0.01$). One-way ANOVA with Tukey's post hoc. Data shown as mean ± S.E.M.

Supplementary tables

Table S1: List of proteins with significantly different relative abundance from somatosensory cortex tissue of Selenate treated animals. One way ANOVA and Tukey's post hoc tets were conducted to identify differences between groups. FDR cutoff of 0.05 was used for significance threshold.

Table S2: List of proteins with significantly different relative abundance from hippocampal tissue of Selenate treated animals. One way ANOVA and Tukey's post hoc tets were conducted to identify differences between groups. FDR cutoff of 0.05 was used for significance threshold.

Table S3: List of ALL metabolites from univariate analysis of untargeted metabolomics data from somatosnery cortex tissue of Selenate treated animals. No metabolites showed significantly different (FDR<0.05) relative abundance between the groups according to one-way ANOVA and Tukey's post hoc test.

Table S4: List metabolites with significantly different relative abundance from hippocampal tissue of Selenate treated animals. One way ANOVA and Tukey's post hoc tets were conducted to identify differences between groups. FDR cutoff of 0.05 was used for significance threshold.

Table S1: List of proteins with significantly different relative abundance from somatosensory cortex tissue of Selenate treated animals.

Uniprot ID	gene	f.value	p.value	FDR
Q5FVJ5	Bmerb1	41.994	2.58E-06	0.014475
F1LUV9	Ncam1	30.015	1.36E-05	0.033682
M0R3N4	Vat1l	28.312	1.80E-05	0.033682
F1M362	Golga7b	25.043	3.24E-05	0.038097
Q66HA8	Hsph1	24.795	3.39E-05	0.038097
F1LR84	Nptx2	23.721	4.18E-05	0.03894
P63086	Mapk1	22.636	5.21E-05	0.03894
O35314	Chgb	21.551	6.55E-05	0.03894
A0A1W2Q6C8	Gfap	21.186	7.09E-05	0.03894
A0A0G2K5N6	Rock2	20.927	7.50E-05	0.03894
P14659	Hspa2	20.827	7.67E-05	0.03894
A0A0G2JW68	Syt6	20.462	8.32E-05	0.03894
Q8VHJ9	nan	19.641	0.0001004	0.042078
D3ZTK0	Ttc9b	19.414	0.00010589	0.042078
P06685	Atp1a1	19.161	0.00011241	0.042078
A0A0G2K014	Lcp1	18.73	0.00012465	0.043044
Q4V7D9	Smpdl3b	18.406	0.00013489	0.043044
P02454	Col1a1	18.276	0.00013925	0.043044
D3ZDH8	Septin5	18.095	0.00014565	0.043044
P07825	Syp	17.302	0.00017808	0.049143
Q5MJ12	Fbxl16	17.083	0.00018848	0.049143
A0A096MJE6	Tnr	16.959	0.00019471	0.049143
A0A0G2K2T8	AABR070542	16.832	0.0002013	0.049143
D3ZDI7	Ppp2r5a	16.666	0.00021038	0.04922

Table S2: List of proteins with significantly different relative abundance from hippocampal tissue of Selenate treated animals.

Uniprot ID	gene	f.value	p.value	FDR
Q0PGW2	Dennd11	61.645	3.64E-07	0.0020148
P47819	Gfap	50.306	1.03E-06	0.0028603
G3V913	Hspb1	45.606	1.70E-06	0.0031382
D3ZRN5	Ro60	28.149	1.85E-05	0.022773
G3V8C3	Vim	27.276	2.15E-05	0.022773
A0A0G2JU96	Ahnak	26.509	2.47E-05	0.022773
A0A0G2JZX9	Pde1a	24.132	3.86E-05	0.0305
A0A0G2JTL4	Kit	22.614	5.23E-05	0.036215
Q6AYC4	Capg	21.236	7.01E-05	0.043127

Table S3: List of ALL metabolites from univariate analysis of untargeted metabolomics data from somatosensory cortex tissue of Selenate treated animals.

Metabolite	**F value**	**P value**	**FDR**
[PI(18:0/20:4)] 1-octadecanoyl-2- (5Z,8Z,11Z,14Z-eicosatetraenoyl)-sn-glycero-3-phospho-(1'-myo-inositol)	21.059	7.29E-05	0.065439
PC(36:4)	13.889	0.00046501	0.14317
Asn-Asn-Gly	12.927	0.00063004	0.14317
N-stearoyl tyrosine	12.365	0.00075846	0.14317
2-Ethylhexyl phthalate	12.217	0.00079718	0.14317
[PC(22:6)]	11.004	0.0012215	0.14613
PS(18:2(9Z,12Z)/22:2(13Z,16 Z))	10.825	0.0013046	0.14613
myo-Inositol 4-phosphate	10.2	0.0016525	0.14613
Neuraminic acid	9.965	0.0018107	0.14613
Methyl (2E,6E)-(10R,11S)-10,11-epoxy-3,7,11-trimethyltrideca-2,6- dienoate	9.8858	0.0018681	0.14613
9S,11R,15S-trihydroxy-5Z,13E-prostadienoic acid- cyclo[8S,12R]	9.8502	0.0018945	0.14613
PS(41:6)	9.42	0.0022523	0.14613
L-Methionine	9.325	0.0023417	0.14613
Ala-Ala-Ala-Asn	9.316	0.0023504	0.14613

4-Acetamidobutanoate	9.0339	0.0026428	0.14613
Taurocyamine	8.7816	0.0029416	0.14613
5,6-Dihydrothymine	8.7197	0.0030208	0.14613
Guanidinoacetate	8.6759	0.0030784	0.14613
5-Guanidino-2- oxopentanoate	8.6657	0.0030919	0.14613
Convicine	8.3463	0.0035559	0.15664
Ascorbate	8.2794	0.0036632	0.15664
L-Threonine	7.9373	0.0042756	0.17452
Ascorbate 2-sulfate	7.5496	0.0051215	0.18685
N-Acetyl-D-mannosaminolactone	7.3299	0.0056882	0.18685
LysoPE(16:0)	7.3088	0.0057465	0.18685
PE(P-36:4)	7.2749	0.0058415	0.18685
L-Tyrosine	7.2519	0.005907	0.18685
L-beta-aspartyl-L-alanine	7.2082	0.0060337	0.18685
N-Pyruvoyl-5-methoxy-3- hydroxyanthranilate	7.1619	0.0061717	0.18685
N-Acetyllactosamine	7.0879	0.0064002	0.18685
Argininicacid	7.072	0.0064504	0.18685
S-Adenosyl-L-homocysteine	6.709	0.0077375	0.21047
Mycolipanolic acid (C24)	6.6883	0.0078196	0.21047
4-coumaroyl-3- hydroxyagmatine	6.6513	0.0079689	0.21047
SM(d38:1)	6.4911	0.0086553	0.22207
Thiamin	6.3828	0.0091588	0.22846
PC(15:0)	6.2634	0.0097547	0.23465

N-Acetyl-D-mannosamine	6.23	0.0099296	0.23465
FA (13:2) tridecadienoic acid	6.0936	0.010683	0.2451
3-Hydroxypropenoate	5.9977	0.011252	0.2451
N-Acetyl-D-glucosamine 6- phosphate	5.8914	0.011927	0.2451
Acanthicifoline	5.8798	0.012003	0.2451
PE(22:5(4Z,7Z,10Z,13Z,16Z)/P 18:1(11Z))	5.869	0.012075	0.2451
N2-Acetyl-L-aminoadipate	5.8359	0.012297	0.2451
Ala-Asp-Gly	5.8126	0.012457	0.2451
PS(14:0/0:0)	5.7984	0.012555	0.2451
L-Asparagine	5.6602	0.013564	0.24801
Mivacurium	5.6595	0.013569	0.24801
PC(30:0)	5.6103	0.013951	0.24801
L-Carnitine	5.5562	0.014386	0.24801
Ala-Gly-Gly-Gly	5.5524	0.014416	0.24801
N-Formimino-L-glutamate	5.5273	0.014625	0.24801
N-Acetyl-D-glucosamine	5.4605	0.015194	0.24801
(R)-3-Hydroxybutanoate	5.4166	0.015583	0.24801
Ala-Asn-Gly	5.406	0.015678	0.24801
PE(36:4)	5.4005	0.015729	0.24801
3-Ethylmalate	5.399	0.015742	0.24801
gamma-L-Glutamyl-L- cysteine	5.3347	0.01634	0.24984
N-acetyl -D- glucosaminitol	5.3268	0.016415	0.24984
L-Phenylalanine	5.2655	0.017013	0.25397
L-Tryptophan	5.2418	0.017252	0.25397
CMP	5.1512	0.018199	0.2572

Met-Ala-Gly	5.1424	0.018294	0.2572
2-Oxobutanoate	5.0911	0.01886	0.2572
PE(34:0)	5.0107	0.019791	0.2572
FA hydroxy(10:0)	5.0014	0.019902	0.2572
Hymexazol O-glucoside	4.9982	0.01994	0.2572
[PS(18:0/20:4)] 1-octadecanoyl-2- (5Z,8Z,11Z,14Z-eicosatetraenoyl)-sn-glycero-3-phosphoserine	4.9919	0.020016	0.2572
Glycyl-leucine	4.9834	0.020119	0.2572
Cys-Lys-Thr-Thr	4.9793	0.020169	0.2572
Glycerophosphoglycerol	4.9542	0.020477	0.2572
Arg-OEt	4.9425	0.020623	0.2572
Vinylacetylglycine	4.9198	0.020908	0.2572
D-Erythrose	4.886	0.021343	0.259
HEPES	4.8296	0.022091	0.25946
Ala-Ala-Ser	4.8138	0.022306	0.25946
propanesulfonate	4.8106	0.02235	0.25946
PC(34:1)	4.7971	0.022537	0.25946
Pyruvate	4.7206	0.023628	0.26858
UDP-D-galactose	4.6938	0.024024	0.26967
Pyrimidodiazepine	4.624	0.025095	0.27238
alpha-D-Galactosyl-N- acetyllactosamine	4.6092	0.025328	0.27238
D-Galactarate	4.6084	0.025342	0.27238
3-Methylbutanamine	4.5998	0.025479	0.27238
PE(P-40:4)	4.5129	0.026917	0.28292
Phe-Asn	4.4805	0.027477	0.28292

ADPribose 2'-phosphate	4.4324	0.028333	0.28292
Ala-Phe-Asp-Tyr	4.4208	0.028545	0.28292
Ala-Ala-Ala	4.3998	0.028932	0.28292
Otonecine	4.3864	0.029182	0.28292
N(pi)-Methyl-L-histidine	4.3741	0.029415	0.28292
LysoPE(18:0)	4.3549	0.029782	0.28292
LysoPE(22:6)	4.3483	0.029908	0.28292
7-Methylguanine	4.3293	0.030279	0.28292
Glu-Asp-Phe	4.3289	0.030286	0.28292
ZAPA	4.3228	0.030407	0.28292
Urea-1-carboxylate	4.315	0.03056	0.28292
LysoPE(20:4)	4.2855	0.031152	0.28545
PS(22:6(4Z,7Z,10Z,13Z,16Z,19 Z)/0:0)	4.2475	0.031935	0.28967
Betaine	4.2136	0.03265	0.2932
N-Formiminoglycine	4.1954	0.033044	0.29379
Homoanserine	4.147	0.034114	0.29688
PS(40:4)	4.1115	0.034927	0.29688
Dephospho-CoA	4.1108	0.034944	0.29688
PC(38:4)	4.1101	0.03496	0.29688
N5-acetyl-N5-hydroxy-L- ornithine	4.1015	0.03516	0.29688
(4R,5S)-4,5,6-Trihydroxy-2,3- dioxohexanoate	4.088	0.035477	0.29688
Chitobiose	4.0784	0.035706	0.29688
N-Carbamyl-L-glutamate	4.0372	0.0367	0.30236
2-amino-2,4-penta-dienoate	3.9919	0.037835	0.30377
Sedoheptulose	3.9916	0.037843	0.30377

Adenine	3.9861	0.037983	0.30377
(2R,4S)-2,4-Diaminopentanoate	3.9697	0.038404	0.30377
D-Glucose	3.9636	0.038563	0.30377
Ala-Leu-Thr-Ala	3.9095	0.040004	0.31238
FA (20:4)	3.865	0.041234	0.31446
3-(Pyrazol-1-yl)-L-alanine	3.8538	0.041551	0.31446
N-(2-hydroxy-docosanoyl)-tetradecasphing-4-enine-1- phosphoethanolamine	3.8507	0.04164	0.31446
N4-Acetylaminobutanal	3.8391	0.041971	0.31446
5'-Methylthioadenosine	3.8374	0.042021	0.31446
N2-(D-1-Carboxyethyl)-L-arginine	3.8183	0.042573	0.31528
Hydantoin-5-propionate	3.7863	0.043522	0.31528
2-Hydroxyethanesulfonate	3.7802	0.043708	0.31528
L-Fuculose 1-phosphate	3.7794	0.04373	0.31528
Tuberonic acid glucoside	3.7742	0.043887	0.31528
Pinidine	3.7555	0.044458	0.31685
D-Histidine	3.7252	0.045403	0.32083
Ile-Thr	3.7148	0.045731	0.32083
D-Asparagine	3.6522	0.047775	0.3295
P-DPD	3.6461	0.04798	0.3295
2-methylhistamine	3.6349	0.048357	0.3295
1-Methylnicotinamide	3.6192	0.048895	0.3295
CoA	3.6181	0.048931	0.3295
3-Hydroxy-N6,N6,N6- trimethyl-L-lysine	3.6112	0.049168	0.3295
Octadecanamide	3.5826	0.050173	0.33201

DG(36:1)	3.5795	0.050282	0.33201
GlcCer(d18:1/23:0)	3.5354	0.051878	0.33921
PE(41:4)	3.5242	0.052291	0.33921
beta-Citryl-L-glutamic acid	3.516	0.052598	0.33921
PC(36:2)	3.4988	0.053245	0.33921
LysoPC(16:0)	3.4984	0.053261	0.33921
CDP-ethanolamine	3.484	0.053811	0.3403
Ergothioneine	3.4694	0.054378	0.34148
3,7,11,15,19,23,27,31,35,39-decamethyltetraconta-2E,6E,10E,14E,18E,22E,26E,30E,34E,38-decaen-1-yl phosphate	3.453	0.05502	0.34311
Ile-Val	3.3915	0.057509	0.35616
N-(6-Aminohexanoyl)-6-aminohexanoate	3.3795	0.058012	0.35682
SM(d18:0/18:1(9Z))	3.3568	0.058975	0.35968
Hypoxanthine	3.3391	0.059741	0.35968
L-Lysine	3.333	0.060004	0.35968
PE(15:0/22:1(13Z))	3.3313	0.06008	0.35968
L-Histidine	3.3123	0.060916	0.36032
L-Leucine	3.3107	0.06099	0.36032
L-Rhamnose	3.292	0.061828	0.36289
[PC(22:6)] 1-(4Z,7Z,10Z,13Z,16Z,19Z-docosahexaenoyl)-sn-glycero-3-phosphocholine	3.2794	0.062402	0.36388
L-Citrulline	3.2491	0.063804	0.36965

D-Glucose 6-phosphate	3.2369	0.06438	0.37048
4-Hydroxybutanoic acid	3.2274	0.064833	0.37048
NADH	3.2172	0.065321	0.37048
N-Acetyl-L-glutamate 5- semialdehyde	3.2072	0.065807	0.37048
FA methyl(12:0) dodecanoic acid	3.203	0.066011	0.37048
FA methyl(6:0)	3.1938	0.066461	0.37069
3-beta-D-Galactosyl-sn- glycerol	3.1775	0.067268	0.37108
3-Methylguanine	3.175	0.067396	0.37108
Rishitin	3.1604	0.068131	0.37108
2-Oxoglutarate	3.1416	0.069089	0.37108
6-oxo-9S,11R,15S-trihydroxy- 13E-prostenoic acid	3.129	0.06974	0.37108
Inumakilactone A glycoside	3.1219	0.070111	0.37108
PE(16:0)	3.1213	0.070146	0.37108
PE(P-38:6)	3.1057	0.070966	0.37108
LysoPE(0:0/22:6(4Z,7Z,10Z,13 Z,16Z,19Z))	3.0944	0.071572	0.37108
PC(20:4)	3.0721	0.072778	0.37108
[SP (24:0)] N-(15Z- tetracosenoyl)-1-beta- glucosyl-sphinganine	3.0707	0.072856	0.37108
Ala-Ala-Asn-Asn	3.054	0.073778	0.37108
3-Fluoro-1-(4-hydroxyphenyl)- 1-propanone	3.0515	0.073918	0.37108
N3-hydroxyethylcytosine	3.0495	0.074029	0.37108
N6,N6,N6-Trimethyl-L-lysine	3.0391	0.074609	0.37108

benzenesulfonate	3.0375	0.074699	0.37108
Creatinine	3.0282	0.075228	0.37108
Asp-Met-Asp-Gly	3.0114	0.076189	0.37108
L-beta-aspartyl-L-threonine	2.9916	0.077343	0.37108
NADP+	2.9827	0.077869	0.37108
D-Ribose	2.9747	0.078343	0.37108
UDP-N-acetyl-D- galactosamine	2.9682	0.078732	0.37108
Ser-Arg	2.9611	0.079158	0.37108
Choline phosphate	2.9523	0.079694	0.37108
FA oxo(10:0)	2.9481	0.079945	0.37108
L-Proline	2.9475	0.079983	0.37108
GDP-3,6-dideoxy-D-galactose	2.9435	0.080227	0.37108
PE(38:6)	2.9376	0.080592	0.37108
ADP	2.9339	0.080819	0.37108
Glucosylceramide (d18:1/24:1(15Z))	2.9327	0.080895	0.37108
gamma-L-Glutamyl-D-alanine	2.9327	0.080895	0.37108
4-Imidazolone-5-propanoate	2.9243	0.081414	0.37108
Galactosylceramide (d18:1/24:1(15Z))	2.9203	0.081667	0.37108
Cer(d36:2)	2.9195	0.081717	0.37108
Nicotinate D-ribonucleoside	2.9127	0.082144	0.37108
FA (8:1)	2.9089	0.082384	0.37108
5-Oxoproline	2.9056	0.082592	0.37108
allopurinol	2.9045	0.082658	0.37108
2-Hydroxybutanoic acid	2.8991	0.083005	0.37108
(S)-piperazine-2-carboxylate	2.8982	0.08306	0.37108

3,4-Dihydroxyphenylacetate	2.8868	0.083791	0.37132
GDP	2.8845	0.08394	0.37132
1-(beta-D-Ribofuranosyl)-1,4-dihydronicotinamide	2.8757	0.084514	0.37182
AMP	2.87	0.084881	0.37182
PE(38:4)	2.862	0.08541	0.37231
Cyclic ADP-ribose	2.8499	0.086212	0.37231
Inosine	2.8411	0.086803	0.37231
trans-Hexadec-2- enoylcarnitine	2.8399	0.086883	0.37231
CMP-N-trimethyl-2-aminoethylphosphonate	2.8372	0.087065	0.37231
ATP	2.8279	0.087689	0.3731
L-Pipecolate	2.8184	0.088343	0.3731
Asp-Met-Cys-Tyr	2.8079	0.089061	0.3731
Phenylpropanoate	2.8077	0.08908	0.3731
Thiomorpholine 3- carboxylate	2.8041	0.089328	0.3731
PE(35:1)	2.7975	0.089789	0.37329
UMP	2.7832	0.090795	0.37354
L-Aspartate 4-semialdehyde	2.7814	0.090921	0.37354
PE(O-38:5)	2.7789	0.091097	0.37354
N-Acetyl-D-fucosamine	2.7575	0.092631	0.37575
Lys-Val	2.7533	0.09294	0.37575
NAD+	2.7508	0.093119	0.37575
D-Arabinonate	2.7482	0.093311	0.37575
[FA methyl(4:1)] 2-methyl-2E- butenoic acid	2.7214	0.095288	0.382

N-acetyl- demethylphophinothricin			
	2.7156	0.095728	0.38206
2-Aminomuconate semialdehyde			
	2.6916	0.097548	0.38338
1-(6-[5]-ladderane-hexanoyl)- 2-(8-[3]-ladderane-octanyl)- sn-glycerol			
	2.6887	0.097777	0.38338
[PI(16:0)] 1-hexadecanoyl-sn- glycero-3-phospho- (1'-myo- inositol)			
	2.6885	0.097791	0.38338
4-Aminobutanoate	2.6883	0.097809	0.38338
Oleoyl-CoA	2.6808	0.09839	0.38338
L-Homocitrulline	2.6755	0.098799	0.38338
Ala-Ser	2.6695	0.099272	0.38338
1-N6-ethenoadenine	2.6591	0.10009	0.38338
Stipitatonate	2.6589	0.1001	0.38338
2-descarboxy-cyclo-dopa	2.6561	0.10033	0.38338
Furfural	2.636	0.10194	0.38512
alpha-aminopimelate	2.6345	0.10206	0.38512
4- Hydroxyphenylacetylglutamic acid	2.6344	0.10207	0.38512
azaguanine	2.6239	0.10293	0.38568
Octadecanoic acid	2.622	0.10308	0.38568
L-Isoleucine	2.6086	0.10419	0.38821
N-Acetyl-L-citrulline	2.5989	0.105	0.38865
5'-methylthioformycin	2.5942	0.10539	0.38865

(3R)-hydroxy-N-acetyl-(L)- arginine			
	2.5917	0.1056	0.38865
Asp-Arg	2.5741	0.10709	0.39154
D-Glucono-1,5-lactone 6- phosphate			
	2.5703	0.10742	0.39154
Dihydroclavaminic acid	2.5587	0.10842	0.39154
LysoPC(20:4)	2.5555	0.10871	0.39154
9-Hexadecenoylcarnitine	2.5527	0.10895	0.39154
L-Serine	2.5518	0.10903	0.39154
(R)-piperidine-3-carboxylate	2.5315	0.11082	0.39154
Cer(d36:1)	2.5314	0.11083	0.39154
Nicotinamide	2.5296	0.11099	0.39154
2-acetamidoglucal	2.5275	0.11118	0.39154
D-Alanyl-D-alanine	2.5269	0.11123	0.39154
CAPS	2.5226	0.11162	0.39154
[FA (22:4)] 7Z,10Z,13Z,16Z-			
docosatetraenoic acid	2.51	0.11276	0.39378
FA (18:1)	2.5059	0.11313	0.39378
(S)-2-Aceto-2-			
hydroxybutanoate	2.4865	0.11492	0.39789
Glu-Arg	2.48	0.11552	0.39789
Pantothenate	2.469	0.11656	0.39789
Homocarnosine	2.4686	0.1166	0.39789
Deoxycytidine	2.4673	0.11672	0.39789
PE(P-38:3)	2.4646	0.11698	0.39789
3-nitro-2-pentanol	2.4595	0.11747	0.39806
Glutathione disulfide	2.4468	0.11868	0.39926
PE(39:4)	2.4465	0.11871	0.39926
Botrydial	2.4388	0.11945	0.40026

Ethanolamine phosphate	2.4335	0.11998	0.40051
Piperidine	2.4204	0.12126	0.4033
(S)-2-Amino-3-(3-hydroxy-4- oxo-4H-pyridin-1-yl)propanoate	2.4024	0.12306	0.40643
D-Xylonate	2.4019	0.1231	0.40643
Cyanidin 3-O-[2''-O-(xylosyl) 6''-O-(p-O-(glucosyl) p- coumaroyl) glucoside] 5-O-[6'''-O-(malonyl) glucoside]	2.3885	0.12446	0.40941
Leu-Ala	2.3704	0.12633	0.41218
GDP-mannose	2.3686	0.12652	0.41218
PE(32:0)	2.367	0.12668	0.41218
Taurine	2.3614	0.12727	0.41225
N6-Acetyl-N6-hydroxy-L- lysine	2.358	0.12762	0.41225
O-Palmitoyl-R-carnitine	2.351	0.12836	0.41315
sn-glycero-3-Phosphocholine	2.3382	0.12972	0.4152
3,4-dehydroproline	2.3363	0.12992	0.4152
Aspartyl-L-proline	2.3238	0.13128	0.41676
Palmitoyl-CoA	2.3232	0.13134	0.41676
PS(44:12)	2.3183	0.13187	0.41697
Thr-Tyr	2.2824	0.13586	0.42807
3-4-DihydroxyphenylglycolO- sulfate	2.2673	0.13757	0.43194
Arecoline	2.26	0.13841	0.43307
Coniine	2.2427	0.14042	0.43718
D-Ribose 5-phosphate	2.2404	0.1407	0.43718

SM(d18:1/24:0)	2.2268	0.1423	0.43731
PA(P-42:4)	2.2267	0.14231	0.43731
Gly-Arg	2.2265	0.14234	0.43731
Swainsonine	2.2236	0.14269	0.43731
Betaine aldehyde	2.2162	0.14356	0.43783
5-methylthiopentylhydroximoyl- cysteinylglycine	2.2007	0.14544	0.43783
N-Acetyl-aspartyl-glutamate	2.1992	0.14563	0.43783
L-Valine	2.1941	0.14625	0.43783
Ile-Lys	2.1939	0.14628	0.43783
4-(Trimethylammonio)but-2-enoate	2.1923	0.14648	0.43783
PC(32:0)	2.1903	0.14672	0.43783
Ne,Ne dimethyllysine	2.19	0.14676	0.43783
PE(39:1)	2.1809	0.14788	0.43972
N6-Methyl-L-lysine	2.1689	0.14938	0.44273
Ile-Gly-Gly	2.1517	0.15157	0.44596
2alpha,7beta,15beta,18- tetraacetoxy-cholest-5-en- 3alpha-ol	2.1497	0.15183	0.44596
N-Acetylmethionine	2.1486	0.15197	0.44596
Riboflavin cyclic-4',5'- phosphate	2.1324	0.15407	0.44828
sn-glycero-3- Phosphoethanolamine	2.1311	0.15424	0.44828
Pro-Arg	2.131	0.15425	0.44828
DIBOA-glucoside	2.1245	0.1551	0.44929
PS(39:4)	2.1078	0.15732	0.45182

Glu-Thr	2.105	0.15769	0.45182
N-Methylhexanamide	2.1048	0.15771	0.45182
2-C-Methyl-D-erythritol 4- phosphate	2.1028	0.15799	0.45182
5-Acetamidopentanoate	2.0893	0.1598	0.45557
N-Acetyl-beta-alanine	2.0845	0.16045	0.45598
3',5'-Cyclic AMP	2.072	0.16218	0.45942
Queuine	2.0619	0.16358	0.45996
PE(34:3)	2.0606	0.16376	0.45996
CHAPS	2.0596	0.1639	0.45996
N6-Acetyl-L-lysine	2.0428	0.16628	0.46087
Val-Arg	2.0355	0.16732	0.46087
N-stearoyl serine	2.0336	0.16759	0.46087
beta-Alanyl-L-arginine	2.0321	0.16781	0.46087
[PE(20:0/15:0)] 1-eicosanoyl- 2-pentadecanoyl-sn-glycero-3 phosphoethanolamine	2.0275	0.16847	0.46087
PC(42:3)	2.0261	0.16867	0.46087
Diethanolamine	2.0226	0.16918	0.46087
MGDG(18:2(9Z,12Z)/18:3(9Z, 12Z,15Z))	2.0178	0.16988	0.46087
Tetradecanoylcarnitine	2.0139	0.17044	0.46087
L-Alanine	2.0081	0.17129	0.46087
FA methyl (8:1)	2.0058	0.17164	0.46087
PS(38:4)	1.9991	0.17263	0.46087
Deoxymannojirimycin	1.9971	0.17293	0.46087
sn-glycerol-1-phosphate	1.9908	0.17386	0.46087
Pantetheine 4'-phosphate	1.9898	0.17402	0.46087

Acetyl-CoA	1.9829	0.17507	0.46087
GDP-L-fucose	1.9786	0.1757	0.46087
CDP-ribitol	1.9765	0.17602	0.46087
3,5/4-Trihydroxycyclohexa- 1,2-dione	1.9719	0.17674	0.46087
N1,N8-diacetylspermidine	1.9718	0.17675	0.46087
9-Oxononanoic acid	1.9709	0.17688	0.46087
N-Ribosylhistidine	1.9695	0.17709	0.46087
[PI(20:4)] 1-(5Z,8Z,11Z,14Z-eicosatetraenoyl)-sn-glycero- 3-phospho-(1'-myo-inositol)	1.9687	0.17721	0.46087
FA hydroxy(18:1)]	1.9667	0.17753	0.46087
Galactosylceramide (d18:1/22:0)	1.9651	0.17777	0.46087
N-hydroxyvaline	1.9628	0.17812	0.46087
α-(2,6-anhydro-3- deoxy-D-arabino-heptulopyranosid)onate 7- phosphate	1.9597	0.1786	0.46087
[SP (24:0)] N-(tetracosanoyl)- 1-beta-glucosyl-sphing-4- enine	1.9593	0.17867	0.46087
gamma-Undecalactone	1.9564	0.17912	0.46087
PS(44:10)	1.9479	0.18043	0.46183
O-Acetylcarnitine	1.9474	0.18052	0.46183
PIPES	1.935	0.18247	0.4642
Coprine	1.9348	0.18249	0.4642

4-Trimethylammoniobutanoate	1.9317	0.18299	0.4642
3-Dehydroxycarnitine	1.9263	0.18384	0.46505
5-Dehydro-4-deoxy-D- glucarate	1.913	0.18598	0.46713
PC(32:1)	1.9123	0.1861	0.46713
Guanosine	1.9115	0.18623	0.46713
Phe-Arg	1.907	0.18696	0.46731
FA hydroxy(7:0)	1.9025	0.18769	0.46731
2-Amino-7,8-dihydro-4-hydroxy-6-(diphosphooxymethyl)pteridi ne	1.9015	0.18786	0.46731
N6-(L-1,3-Dicarboxypropyl)-L- lysine	1.8961	0.18874	0.46752
PE(18:3(6Z,9Z,12Z)/P- 18:1(11Z))	1.8946	0.18899	0.46752
Cer(d-h 35:0)	1.8902	0.18972	0.46783
2-Methylcholine	1.8869	0.19027	0.46783
O-Propanoylcarnitine	1.8813	0.19119	0.46783
UDP	1.8813	0.1912	0.46783
L-Cysteate	1.8707	0.19297	0.4709
Asp-Gln	1.8665	0.19369	0.47136
N3-(4-methoxyfumaroyl)-L-2,3-diaminopropanoate	1.8615	0.19455	0.47217
formiminoalanine	1.8522	0.19613	0.47361
IMP	1.8518	0.19619	0.47361
[PR] Vitamin E	1.848	0.19686	0.47394
L-Lathyrine	1.8434	0.19765	0.47456

Hydroxyhexanoycarnitine	1.8349	0.19913	0.47537
D-Sedoheptulose 7- phosphate	1.832	0.19964	0.47537
Asn-Met-Gln-Ser	1.829	0.20016	0.47537
2,5-Dioxopentanoate	1.8277	0.20039	0.47537
Sulfate	1.8246	0.20093	0.47537
glycerophosphoserine	1.8234	0.20116	0.47537
(S)-Malate	1.8137	0.20288	0.47818
4-Guanidinobutanoate	1.8032	0.20477	0.48118
Oleoylcarnitine	1.8006	0.20523	0.48118
Ganglioside GD3 (d18:1/18:0)	1.7815	0.20872	0.48811
PC(35:4)	1.7725	0.21039	0.48976
N6-Acetyl-LL-2,6-diaminoheptanedioate	1.7707	0.21073	0.48976
Mescaline	1.7689	0.21106	0.48976
N-Acetyl-L-2-amino-6- oxopimelate	1.7634	0.21209	0.49087
Succinyladenosine	1.7507	0.2145	0.4932
NADPH	1.7503	0.21458	0.4932
PC(40:2)	1.7468	0.21525	0.4932
Citrate	1.7465	0.21529	0.4932
PI(38:4)	1.74	0.21654	0.49337
Phytuberin	1.7398	0.21659	0.49337
L-Aspartate	1.7375	0.21702	0.49337
(R)-piperazine-2-carboxylate	1.7347	0.21757	0.49337
2,3-Diaminosalicylic acid	1.7301	0.21847	0.49416
4-Methylene-L-glutamate	1.7228	0.21987	0.49609

Glu-Met-Met	1.711	0.22221	0.49664
5-Methyl-2'-deoxycytidine	1.7057	0.22326	0.49664
γ-aminobutyramide	1.705	0.22341	0.49664
(2R,4R)-1,2,7,7-tetramethylbicyclo[2.2.1]hep tan-2-ol	1.7038	0.22363	0.49664
Thiamin monophosphate	1.7007	0.22426	0.49664
Acetylpyruvate	1.7002	0.22437	0.49664
Sarmentosin epoxide	1.6974	0.22492	0.49664
[PR] bacteriohopane-,32,33,34-triol-35-cyclitolguanine	1.695	0.22539	0.49664
3'-CMP	1.6941	0.22559	0.49664
Daminozide	1.6914	0.22613	0.49664
Val-Val	1.6911	0.2262	0.49664
Xanthosine	1.684	0.22763	0.49857
N-Nonanoylglycine	1.679	0.22866	0.49959
sn-glycero-3-Phospho-1-inositol	1.6658	0.23138	0.50431
N-Undecanoylglycine	1.6617	0.23221	0.50435
TG(45:4)	1.6603	0.23252	0.50435
Phosphocreatine	1.6546	0.23371	0.50571
FA hydroxy(8:0) hydroxy- octanoic acid	1.6517	0.23431	0.50574
Arg-Glu-Ile-Phe	1.6475	0.23519	0.50574
L-2-Amino-3-oxobutanoic acid	1.6463	0.23545	0.50574
Gamma-Aminobutyryl-lysine	1.6431	0.23613	0.50574

3-Butynoate	1.6407	0.23664	0.50574
L-Hypoglycin	1.6381	0.23719	0.50574
PC(33:1)	1.6309	0.23873	0.50574
Asp-Cys-Cys-Ser	1.6277	0.23942	0.50574
S-Adenosyl-L-methionine	1.6204	0.241	0.50574
D-myo-Inositol 1,2-cyclic phosphate	1.6199	0.24111	0.50574
[FA (6:0)] hexanal	1.6195	0.24121	0.50574
DG(38:5)	1.6159	0.24199	0.50574
PS(18:0/18:1(9Z))	1.6118	0.24288	0.50574
Ala-Asp-Cys	1.6101	0.24325	0.50574
PE(35:0)	1.6085	0.24359	0.50574
PC(34:0)	1.6068	0.24398	0.50574
Crotonoside	1.6067	0.24399	0.50574
FA methyl(8:0)	1.6064	0.24406	0.50574
His-Phe-Phe-Pro	1.6048	0.24442	0.50574
Lys-Met-Phe-Phe	1.601	0.24525	0.50629
N-(2-hydroxy-tetracosanoyl)- hexadecasphing-4-enine-1- phosphoethanolamine	1.5985	0.24582	0.50629
Ethyl (R)-3-hydroxybutanoate	1.5923	0.2472	0.50798
Mannitol	1.5886	0.24802	0.50849
Glycerol	1.586	0.2486	0.50853
Kurilensoside G	1.582	0.2495	0.50921
PE(22:1(13Z)/15:0)	1.5762	0.25082	0.51073
dAMP	1.5649	0.25339	0.51129
[PA(16:0/0:0)] 1-hexadecanoyl-2-sn-glycero-3- phosphate	1.5635	0.25372	0.51129

Acetyl phosphate	1.5628	0.25388	0.51129
N2-Succinyl-L-ornithine	1.5592	0.25471	0.51129
PC(42:10)	1.5587	0.25483	0.51129
N6-(1,2-Dicarboxyethyl)-AMP	1.5578	0.25505	0.51129
D-Ribulose 5-phosphate	1.5576	0.25507	0.51129
3-Methylbutanoic acid	1.5456	0.25788	0.51576
PC(31:1)	1.5411	0.25893	0.5167
amiclenomycin	1.5275	0.26215	0.52098
GalCer(d18:2/23:0)	1.5272	0.26224	0.52098
PS(O-36:2)	1.5226	0.26332	0.52098
L-isoleucyl-L-proline	1.5206	0.26381	0.52098
Boc-Asn	1.5199	0.26397	0.52098
D-Gluconic acid	1.5158	0.26497	0.52181
Guanine	1.5025	0.2682	0.527
N-Acetylcystathionine	1.4892	0.27147	0.5315
Tetradecanoic acid	1.4884	0.27167	0.5315
L-Canaline	1.4828	0.27306	0.53205
[PC(14:0/18:0)] 1-tetradecanoyl-2-octadecanoyl-sn-glycero-3-phosphocholine	1.4784	0.27417	0.53205
Glucosylceramide (d18:1/22:0)	1.4734	0.27542	0.53205
1-Aminocyclopentanecarboxylate	1.473	0.27553	0.53205
5-diazo-4-oxo-norvaline	1.4707	0.27613	0.53205
O-Butanoylcarnitine	1.469	0.27654	0.53205

2-5-Furandicarboxylicacid	1.463	0.27807	0.53205
CAI-1	1.4617	0.27841	0.53205
N-Carboxyethyl-g- aminobutyricacid	1.4609	0.2786	0.53205
PA(O-33:1)	1.4608	0.27863	0.53205
N-Acetyl-O-acetylneuraminate	1.459	0.27909	0.53205
4-methylhistamine	1.4573	0.27953	0.53205
PE(P-40:6)	1.455	0.28011	0.53205
Pirbuterol	1.4545	0.28024	0.53205
[SP] Sphing-4-enine-1- phosphate	1.4473	0.28211	0.53404
7-Hydroxy-3-(4- methoxyphenyl)-4-propyl-2H- 1-benzopyran-2-one	1.4431	0.28319	0.53404
2,7-Anhydro-alpha-N- acetylneuraminic acid	1.4414	0.28364	0.53404
2-Oxoglutaramate	1.4413	0.28367	0.53404
FA hydroxy(9:0) hydroxy- nonanoic acid	1.4312	0.28631	0.53788
L-2,4-Diaminobutanoate	1.4274	0.28732	0.53814
Glutathione	1.4261	0.28765	0.53814
6-methyltetrahydropterin	1.4205	0.28915	0.53982
Ile-Ala-Gly	1.4181	0.28978	0.53988
LysoPE(18:1)	1.4088	0.29227	0.54304
2,3-Dimethylmaleate	1.4063	0.29296	0.54304
PE(43:6)	1.4031	0.29381	0.54304
Ala-Phe-Tyr-Tyr	1.4011	0.29436	0.54304

PC(38:6)	1.4006	0.2945	0.54304
gamma-Amino-gamma- cyanobutanoate			
	1.3958	0.29582	0.54435
Dihydrobiopterin	1.3845	0.29891	0.54745
sodium dodecyl sulfate	1.3823	0.29952	0.54745
FA (8:0) octanoic acid	1.3822	0.29953	0.54745
L-beta-aspartyl-L-leucine	1.3808	0.29994	0.54745
Arachidonyl-CoA	1.377	0.30098	0.54823
L-beta-aspartyl-L- glutamicacid			
	1.3719	0.30242	0.54975
PE(39:2)	1.3697	0.30304	0.54975
3-Methyl-2-oxobutanoic acid	1.3606	0.30558	0.55218
[SP] (3'-sulfo)Galbeta- Cer(d42:2)			
	1.3604	0.30565	0.55218
FA hydroxy(6:0)	1.3558	0.30695	0.55218
LysoPE(22:4)	1.3554	0.30707	0.55218
4-Guanidinobutanal	1.3541	0.30745	0.55218
PE(19:0)	1.3446	0.31016	0.55594
(S)-piperazine-2-carboxamide	1.3388	0.31184	0.55754
6-diazo-5-oxonorleucine	1.3317	0.31388	0.55754
[ST hydrox] 3alpha,7alpha- Dihydroxy-5beta- cholan-24- oic Acid			
	1.3314	0.31397	0.55754
Gamma-Glutamylglutamine	1.3294	0.31456	0.55754
2-Hydroxyethylphosphonate	1.3278	0.31504	0.55754
sn-Glycerol 3-phosphate	1.3266	0.3154	0.55754
Homoarginine	1.3236	0.31626	0.55754

[FA amino(14:0)] 2-amino- tetradecanoic acid			
	1.323	0.31644	0.55754
S-Acetyldihydrolipoamide	1.3223	0.31664	0.55754
Lys-Gly-Pro-Pro	1.3126	0.31953	0.56043
PS(O-20:0/0:0)	1.3126	0.31953	0.56043
[FA trihydroxy(4:0)] 2,3,4- trihydroxy-butanoic			
acid	1.2999	0.32332	0.56507
Glucosylceramide	1.2995	0.32344	0.56507
FA (20:1)	1.2916	0.32582	0.56813
D-Glucono-1,5-lactone	1.289	0.32663	0.56813
FA oxo(7:0)	1.2875	0.32709	0.56813
Turgorin	1.2761	0.33057	0.57308
γ-glutamyl-L- alaninol			
	1.2713	0.33206	0.57455
FA (17:0)	1.2673	0.33331	0.57543
(3R)-oct-1-en-3-ol	1.2655	0.33386	0.57543
Hexose phosphate	1.2619	0.33499	0.57543
Bis(2-ethylhexyl)phthalate	1.2593	0.33581	0.57543
CDP-choline	1.2575	0.3364	0.57543
3-Guanidinopropanoate	1.2574	0.33642	0.57543
SM(d34:1)	1.2539	0.33752	0.57623
3-Dehydroquinate	1.2416	0.34141	0.58069
Ile-Ser	1.2416	0.34143	0.58069
Methylimidazole acetaldehyde			
	1.2354	0.34342	0.58297
3,5,7-Trimethyl-2E,4E,6E,8E-			
undecatetraene	1.2303	0.34505	0.58323
[SP] (3'-sulfo)Galbeta- Cer(d18:1/24:1(15Z))			
	1.2297	0.34526	0.58323

Decanoic acid	1.2289	0.34552	0.58323
FA(16:1)	1.2223	0.34765	0.58509
PC(40:6)	1.2215	0.34793	0.58509
Fibrin	1.2164	0.3496	0.58681
Hexanoylcarnitine	1.2128	0.35077	0.58766
1-O-Methyl-myo-inositol	1.201	0.35469	0.59273
Glu-Glu	1.1996	0.35515	0.59273
5-6-Dihydrouridine	1.1977	0.35577	0.59273
1-(4-amino-2-methylpyrimid- 5-ylmethyl)-3- (β- hydroxyethyl)-2- methylpyridinium bromide	1.1925	0.35752	0.59454
chromate	1.1898	0.35845	0.59499
Uracil	1.1831	0.36071	0.59687
Ala-Pro	1.1825	0.36091	0.59687
LysoPE(0:0/20:4(5Z,8Z,11Z,14 Z))	1.1798	0.36183	0.59728
[PE(16:1)] 1-(1Z-hexadecenyl)- sn-glycero-3- phosphoethanolamine	1.1726	0.36428	0.60023
N-Methyltyramine	1.1673	0.36613	0.60089
PA(O-36:2)	1.1661	0.36651	0.60089
Ile-Arg	1.1647	0.367	0.60089
PE(P-42:0)	1.1637	0.36736	0.60089
PS(34:1)	1.1569	0.36972	0.60235
Ganglioside GM2 (d36:1)	1.1543	0.37061	0.60235
FA (9:2) nonadienoic acid	1.1474	0.37304	0.60235
trans-4- Hydroxycyclohexanecarboxyl ate			

	1.1464	0.37339	0.60235
1-(3-aminopropyl)-4- aminobutanal			
	1.1451	0.37385	0.60235
D-Fructose 1,6-bisphosphate	1.1451	0.37386	0.60235
PG(38:4)	1.1418	0.37504	0.60235
Barbiturate	1.1416	0.37508	0.60235
(-)-Camphor	1.138	0.37638	0.60235
[SP] (3'-sulfo)Galbeta- Cer(dOH-42:1)			
	1.1364	0.37696	0.60235
ADP-ribose	1.1359	0.37712	0.60235
PS(P-37:2)	1.1358	0.37716	0.60235
Dodecanoylcarnitine	1.1319	0.37857	0.60235
D-Erythrose 4-phosphate	1.1286	0.37975	0.60235
L-Arginine	1.1267	0.38041	0.60235
PC(P-38:0)	1.125	0.38103	0.60235
N-(docosanoyl)-sphinganine-1- phospho-(1'-myo-inositol)	1.1234	0.3816	0.60235
7-oxoheptanoate	1.1219	0.38213	0.60235
11'-Carboxy-alpha-chromanol	1.1217	0.38223	0.60235
(S)-Lactate	1.1209	0.38251	0.60235
Adenosine	1.1208	0.38253	0.60235
D-Glutamate	1.1195	0.38301	0.60235
Orthophosphate	1.1096	0.38663	0.60698
Ile-Asn	1.1052	0.38825	0.60846
8-Hydroxypurine	1.1013	0.38967	0.60963
Hydroxypyruvate	1.0993	0.3904	0.60971
1-butanesulfonate	1.0915	0.3933	0.61316

3-deoxy-D-galactose	1.089	0.39425	0.61359
Leu-Ser	1.0823	0.39674	0.61639
L-threonine amide	1.0776	0.39852	0.61767
Ile-Ala	1.0742	0.3998	0.61767
N-Acetyl-D-glucosamine 4- sulfate	1.0726	0.40043	0.61767
Galegine	1.0714	0.40086	0.61767
PS(0-36:1)	1.0711	0.401	0.61767
Embelin	1.0644	0.40353	0.62049
Urocanate	1.0577	0.4061	0.62264
PA(38:4)	1.0568	0.40646	0.62264
Cytidine	1.0534	0.40778	0.62264
Thymine	1.049	0.4095	0.62264
1-Methyl-4-phenyl-1,2,3,6- tetrahydropyridine N-oxide	1.0462	0.41057	0.62264
1,2-Dihydroxymint lactone	1.0456	0.41083	0.62264
Ala-Thr-Ala-Ser	1.045	0.41103	0.62264
Pentanamide	1.0447	0.41116	0.62264
Eugenol methyl ether	1.0447	0.41117	0.62264
(R)-2-Hydroxyglutarate	1.0395	0.4132	0.62314
Acetylenedicarboxylate	1.0388	0.41349	0.62314
PE(15:0/20:0)	1.0385	0.41358	0.62314
octulose 8-phosphate	1.0364	0.41443	0.62338
PE(42:2)	1.0322	0.41607	0.62411
[ST (3:0)] 26-O-[beta-D-glucopyranosyl]-25R-furostan- 3beta,22alpha,26-triol	1.0316	0.4163	0.62411
N-α-L-histidine	1.0272	0.41805	0.62569

FA (14:2) tetradecadienal	1.0243	0.41921	0.62638
N-(2-hydroxy-tetracosanoyl)- 1-beta-glucosyl-tetradecasphing-4-enine	1.0204	0.42077	0.62679
N-α-acetyl lysine methyl ester	1.0201	0.42089	0.62679
N-acetyl-(L)-arginine	1.0163	0.42241	0.62705
DG(32:0)	1.0162	0.42246	0.62705
XDP	1.0138	0.42343	0.62746
Orotate(Fragment)	1.0093	0.42526	0.62913
(1R,2S)-1-Hydroxypropane- 1,2,3-tricarboxylate	1.0063	0.42647	0.62954
PA(34:1)	1.0046	0.42714	0.62954
(1-Ribosylimidazole)-4- acetate	1.0026	0.42797	0.62954
SM(d36:1)	1.0017	0.42834	0.62954
N-Formyl-L-methionine	0.99748	0.43006	0.63003
L-Homocysteic acid	0.996	0.43067	0.63003
perchlorate	0.99574	0.43078	0.63003
Leu-Pro	0.98801	0.43396	0.63365
FA oxo(9:0) oxo-nonanoic acid	0.98492	0.43524	0.63449
Graphinone	0.97689	0.43858	0.63784
Isonicotineamide	0.976	0.43896	0.63784
[FA tetramethyl(4:0/11:0/2:0)] 2,2,9,9-tetramethyl-undecan- 1,10-diol	0.96728	0.44262	0.64212
Muscimol	0.9641	0.44397	0.64304
PS(36:1)	0.9554	0.44767	0.6453

3-Phospho-D-glycerate	0.9545	0.44805	0.6453
PE(40:6)	0.95382	0.44835	0.6453
Carnosine	0.95367	0.44841	0.6453
PE(34:1)	0.94904	0.45039	0.64713
N3-methylcytosine	0.94653	0.45148	0.64733
Poly-N-acetyllactosamine	0.9445	0.45235	0.64733
Brunfelsamidine	0.94117	0.45379	0.64733
Deoxyadenosine	0.94117	0.45379	0.64733
SM(d16:1/20:0)	0.9389	0.45477	0.64733
Isoamyl formate	0.93639	0.45587	0.64733
N-Acetylglutamine	0.93597	0.45605	0.64733
FAD	0.93538	0.4563	0.64733
beta-Alanyl-L-lysine	0.93106	0.45819	0.64898
Thr-Arg	0.92514	0.46079	0.65001
GMP	0.92412	0.46124	0.65001
N-Acetyl-L-histidine	0.92367	0.46144	0.65001
1-Hexadecylthio-2- hexadecanoylamino-1,2-dideoxy-sn-glycero-3- phosphocholine	0.92188	0.46223	0.65001
S-2,3-dicarboxyaziridine	0.91886	0.46357	0.65001
L-Ornithine	0.91835	0.46379	0.65001
4-Toluenesulfonamide	0.91675	0.4645	0.65001
Glycylproline	0.91629	0.46471	0.65001
5-exo-Hydroxy-1,2- campholide	0.91387	0.46578	0.6505
Sucrose	0.91198	0.46662	0.65066
4-Methyl-2-oxopentanoate	0.90997	0.46752	0.65079
3-Oxopropanoate	0.90771	0.46853	0.65079

D-Mycinose	0.90691	0.46889	0.65079
Allysine	0.90276	0.47075	0.65237
Phosphodimethylethanolamine	0.89999	0.472	0.65256
[SP](3'-sulfo)Galbeta- Cer(d18:0/2-OH-24:0)	0.89923	0.47234	0.65256
PI(38:6)	0.89311	0.47511	0.65538
S-carboxymethyl-D-cysteine	0.88646	0.47814	0.65855
trans-Aconitate	0.88434	0.47912	0.65888
DG(38:4)	0.87735	0.48233	0.66193
Ala-Gly-Pro	0.8763	0.48281	0.66193
FA(22:5)	0.87312	0.48428	0.66212
Peonidin	0.87123	0.48516	0.66212
PI(40:6)	0.87122	0.48516	0.66212
N-Stearoylsphingosine	0.86885	0.48626	0.66262
3-(Uracil-1-yl)-L-alanine	0.86476	0.48817	0.66421
Asn-Lys-Asn-Pro	0.86279	0.48909	0.66445
L-Albizziine	0.85948	0.49064	0.66556
(1R,4S)-fenchan-2-one	0.85789	0.49139	0.66557
2-Hydroxymalonate	0.85452	0.49297	0.6667
L-Dehydroascorbate	0.85221	0.49407	0.66718
2-Hydroxyadenine	0.84175	0.49903	0.67287
Hypotaurine	0.83831	0.50068	0.67408
Asn-Met-Gln-Pro	0.83224	0.5036	0.67699
alpha-Methylstyrene	0.82707	0.50609	0.67913
SM(d40:1)	0.82581	0.5067	0.67913
Succinate	0.81463	0.51215	0.6848
N2-Acetyl-L-lysine	0.81257	0.51316	0.6848

[PR] (+)-Bornane-2,5-dione	0.81245	0.51322	0.6848
D-Mannonate	0.80751	0.51565	0.68702
PS(15:0)	0.79579	0.52146	0.69374
PC(P-40:0)	0.7929	0.5229	0.69463
Monomethyl sulfate	0.78637	0.52618	0.69718
[FA (10:0/2:0)] Decanedioic acid	0.78598	0.52638	0.69718
Urate	0.77831	0.53025	0.70127
TG(48:5)	0.77501	0.53193	0.70173
Ganglioside GM3 (d18:1/18:0)	0.77433	0.53227	0.70173
[PS(18:1)] 1-(9Z-octadecenoyl)-sn-glycero-3- phosphoserine	0.77301	0.53294	0.70173
PC(17:0/14:1)	0.76738	0.53582	0.70449
Uridine	0.76357	0.53777	0.70602
N-Sulfo-D-glucosamine	0.76159	0.53879	0.70633
L-histidine hydroxamate	0.75458	0.54241	0.71004
3-ureidoacrylate	0.74816	0.54575	0.71337
Pyrophosphate	0.7426	0.54865	0.71612
PC(P-33:1)	0.74	0.55002	0.71686
Retronecine	0.73543	0.55242	0.71895
Proacaciberin	0.73019	0.55519	0.72049
Anhydrotetracycline	0.73016	0.55521	0.72049
LysoPC(18:0)	0.72192	0.55959	0.72315
L-2,3-Diaminopropanoate	0.7212	0.55997	0.72315
DG(34:1)	0.71885	0.56123	0.72315
Nalpha-Methylhistidine	0.71826	0.56155	0.72315

N1-Methyl-2-pyridone-5- carboxamide			
	0.71763	0.56188	0.72315
O-Acetyl-L-homoserine	0.71725	0.56209	0.72315
5-Methylcytidine	0.71278	0.56449	0.7252
FA oxo(8:0) oxo-octanoic acid	0.70592	0.56819	0.72891
PE(P-38:2)	0.70033	0.57123	0.73176
2'-O-Methyladenosine	0.69865	0.57214	0.73188
N-carbamoylglycine	0.69589	0.57365	0.73207
3-(4-Hydroxyphenyl)lactate	0.69423	0.57456	0.73207
DG(44:11)	0.69391	0.57473	0.73207
3-Deoxy-D-manno- octulosonate 8-phosphate			
	0.68755	0.57822	0.73547
LysoPC(16:1(9Z))	0.68462	0.57984	0.73584
2-Aminoacrylate	0.6831	0.58068	0.73584
Ngamma-Monomethyl-L- arginine			
	0.68088	0.58191	0.73584
SM(d18:1/18:0)	0.68077	0.58197	0.73584
a Cysteine adduct	0.67961	0.58261	0.73584
N-Acetyl-L-aspartate	0.67424	0.58559	0.73795
N-Acetylneuraminate	0.67365	0.58592	0.73795
PC(o-44:5)	0.66642	0.58996	0.742
FA (18:2)	0.66061	0.59323	0.74506
[PA(16:0/18:1)] 1- hexadecanoyl-2-(11Z- octadecenoyl)-sn-glycero- 3- phosphate			
	0.65669	0.59544	0.7468
FA hydroxy(12:1)	0.65106	0.59863	0.74757
[FA (11:0)] undecanoic acid	0.64903	0.59978	0.74757

PA(36:4)	0.64859	0.60004	0.74757
PS(38:1)	0.64843	0.60013	0.74757
Ganglioside GM1 (18:1/9Z- 18:1)	0.64749	0.60066	0.74757
FA (8:1) octenal	0.64681	0.60105	0.74757
Deoxyuridine	0.63153	0.60982	0.75742
hexanesulfonate	0.62832	0.61168	0.75868
Glycerone phosphate	0.62291	0.61481	0.76141
Pseudouridine	0.6216	0.61558	0.76141
Asp-Pro-Pro-Tyr	0.6189	0.61715	0.7621
4-Hydroxyhexan-3-one	0.61775	0.61782	0.7621
Hydroxybutyrylcarnitine	0.61283	0.62071	0.7646
L-Glutamine	0.60972	0.62253	0.76486
PS(40:6)	0.60957	0.62262	0.76486
Cys-Cys-Gly-Tyr	0.60555	0.62498	0.76672
N-Methylhistamine	0.6024	0.62685	0.76772
2-isocapryloyl-3R- hydroxymethyl-γ-butyrolactone	0.60124	0.62754	0.76772
Hydroxymethylphosphonate	0.59984	0.62837	0.76772
FA methyl(14:0)	0.59812	0.62938	0.76792
PC(o- 22:0/20:4(8Z,11Z,14Z,17Z))	0.59148	0.63334	0.77093
PE(P-36:1)	0.59044	0.63396	0.77093
PS(16:0/22:1(11Z))	0.58966	0.63443	0.77093
Tetraethylammonium	0.58702	0.63601	0.7718
Imidazole-4-methanol	0.58273	0.63858	0.77388
PS(O-34:0)	0.57923	0.64068	0.77538
PE(41:6)	0.57456	0.6435	0.77775

3-ketothreonine	0.57181	0.64517	0.77871
Octylamine	0.57003	0.64625	0.77897
N-Carbamoylsarcosine	0.567	0.64809	0.77973
[SP (22:0)] N-(docosanoyl)-1- beta-glucosyl-sphinganine	0.56614	0.64861	0.77973
SM(d37:1)	0.55435	0.65582	0.78702
Orotate	0.55336	0.65643	0.78702
PA(P-35:2)	0.54877	0.65926	0.78928
PC(42:2)	0.54735	0.66013	0.78928
[FA amino(4:0)] 2-amino-4- cyano-butanoic acid	0.54603	0.66095	0.78928
1-(3,4-dimethoxylphenyl)ethane-1,2- diol	0.54186	0.66354	0.79131
Benzimidazole	0.54043	0.66442	0.79131
[FA (18:1)] 9Z-octadecenamide	0.5377	0.66612	0.79228
[LysoPC(16:2)] 1-hexadecyl-sn- glycero-3-phosphocholine	0.53526	0.66763	0.79254
Linoleamide	0.53451	0.6681	0.79254
5-Hydroxyindoleacetate	0.5181	0.67839	0.80369
N4-(Acetyl-beta-D- glucosaminyl)asparagine	0.51434	0.68077	0.80457
L-cycloserine	0.51191	0.68231	0.80457
PE(18:1)	0.51032	0.68332	0.80457
Glu-Cys-Gly	0.51008	0.68347	0.80457
Fagomine	0.50984	0.68362	0.80457
Methylisoeugenol	0.50493	0.68674	0.8063

PC(P-36:1)	0.5047	0.68689	0.8063
Dodecanoic acid	0.50221	0.68847	0.80667
D-Arabitol	0.5014	0.68899	0.80667
FA (14:1)nonanoic acid	0.49509	0.69303	0.80871
GlcCer(d18:2/23:0)	0.495	0.69308	0.80871
Ophthalmicacid	0.49304	0.69434	0.80871
cis-5-Tetradecenoylcarnitine	0.49182	0.69513	0.80871
Glutarylcarnitine	0.49164	0.69524	0.80871
PC(18:0)	0.48293	0.70085	0.81317
[SP (18:0)] N-(octadecanoyl)- sphing-4-enine	0.48288	0.70089	0.81317
3-O-Sulfogalactosylceramide(d18	0.4776	0.70431	0.81427
PE(37:1)	0.47751	0.70436	0.81427
2-Hydroxy-2,4-pentadienoate	0.47657	0.70497	0.81427
Methylenediurea	0.47581	0.70546	0.81427
PE(36:2)	0.46881	0.71002	0.81848
N-hydroxyisoleucine	0.46581	0.71198	0.81899
Elaidamide	0.46455	0.7128	0.81899
2-O-Methylcytosine	0.46298	0.71383	0.81899
Aminomalonate	0.46183	0.71458	0.81899
5'-deoxy-5'-fluoroadenosine	0.46116	0.71502	0.81899
Erythronicacid	0.45963	0.71602	0.81909
Hexadecanoic acid	0.45025	0.72219	0.8251
2alpha-Methyl-17beta- [(tetrahydro-2H-pyran-2- yl)oxy]-5alpha- androstan-3- one	0.44663	0.72458	0.82678

Homostachydrine	0.44408	0.72626	0.82765
PI(36:4)	0.44201	0.72763	0.82789
FA amino(18:0)	0.44098	0.72832	0.82789
Tetranor-PGE1	0.43875	0.7298	0.82852
Glucosylceramide (d18:1/20:0)	0.43602	0.73161	0.82871
2-AminoAMP	0.43571	0.73181	0.82871
[FA (16:2)] N-hexadecyl- ethanolamine	0.43298	0.73363	0.82973
Picolinamide	0.42722	0.73748	0.83302
L-proline amide	0.42581	0.73842	0.83304
PIP(38:4)	0.42203	0.74095	0.83413
PC(O-42:6)	0.42029	0.74211	0.83413
Choline	0.42021	0.74217	0.83413
PC(42:7)	0.41643	0.74471	0.83593
PC(36:1)	0.41279	0.74715	0.83763
LysoPC(18:1)	0.41002	0.74902	0.83868
β-cyano-L-alanine	0.40607	0.75168	0.84033
Iminoaspartate	0.40399	0.75309	0.84033
2-(alpha-Hydroxyethyl)thiamine diphosphate	0.40367	0.7533	0.84033
2,3,6-Trihydroxypyridine	0.39719	0.75769	0.84418
17beta-Hydroxy-6beta- methyl-5alpha-androstan-3- one propionate	0.39269	0.76075	0.84653
Cimifugin	0.3797	0.7696	0.85532
Slaframine	0.37687	0.77154	0.85618

2-Methylbutyroylcarnitine	0.37545	0.7725	0.85618
(R)-AMAA	0.3744	0.77323	0.85618
L-Histidinol	0.3707	0.77576	0.85792
L-Methionine S-oxide	0.36607	0.77894	0.86038
DG(P-32:1)	0.36293	0.7811	0.86171
Acetylcholine	0.3588	0.78394	0.86365
CL(20:2(11Z,14Z)/18:2(9Z,12 Z)/18:2(9Z,12Z)/18:2(9Z,12Z))	0.35643	0.78558	0.86365
Lotaustralin	0.35618	0.78575	0.86365
[PI(18:1)] 1-(9Z- octadecenoyl)-sn-glycero-3- phospho-(1'-myo- inositol)	0.35265	0.78819	0.86527
PS(38:2)	0.35005	0.78998	0.86618
[PG (18:1)] 1-(9E- octadecenoyl)-sn-glycero-3- phospho-(1'-sn- glycerol)	0.34538	0.79321	0.868
PC(18:1)	0.34486	0.79357	0.868
Ile-Lys-Pro	0.33826	0.79814	0.87194
SM(d18:0/18:1(11Z))	0.3335	0.80144	0.8734
Propanoyl phosphate	0.33311	0.80171	0.8734
N-Acetylornithine	0.33211	0.8024	0.8734
PE(O-36:3)	0.32955	0.80418	0.87371
LysoPC(20:1)	0.32891	0.80463	0.87371
Formylpyruvate	0.32397	0.80806	0.87638
[FA oxo(8:1)] 5-oxo-7- octenoic acid	0.31745	0.8126	0.87957
5,6-Dihydrouracil	0.31693	0.81296	0.87957
aminoacrylate	0.3152	0.81417	0.87981

3-Amino-2-piperidone	0.30856	0.8188	0.88359
6-Phospho-D-gluconate	0.30736	0.81963	0.88359
PG(42:10)	0.29477	0.82842	0.892
dihydrothymidine	0.28674	0.83404	0.89696
FMN	0.27868	0.83967	0.90147
PE(P-34:1)	0.27787	0.84024	0.90147
[SP] (3'-sulfo)Galbeta- Cer(d18:0/2-OH-22:0)	0.27286	0.84373	0.90414
L-Glutamate methylester	0.265	0.84922	0.90888
N-Acetyl-beta-D- glucosaminylamine	0.26272	0.85082	0.90888
PA(40:2)	0.26135	0.85178	0.90888
3-(2-propenoic acid)-4,6- hydroxy cyclohexa-2,5-dienone	0.26074	0.8522	0.90888
PG(34:1)	0.25856	0.85372	0.90942
PE(P-40:0)	0.25493	0.85625	0.91104
3-Methoxy-4- hydroxyphenylethyleneglycol sulfate	0.23433	0.87058	0.92444
Procollagen 5-(D- galactosyloxy)-L-lysine	0.23385	0.87091	0.92444
1-(14-methyl-pentadecanoyl)- 2-(8-[3]-ladderane-octanyl)- sn-glycerol	0.22625	0.87618	0.92893
PC(18:2)	0.21918	0.88106	0.93301
dCDP-ethanolamine	0.21571	0.88345	0.93355
PE(36:1)	0.21542	0.88365	0.93355
PC(40:1)	0.21108	0.88663	0.9356

CMP-N-acetylneuraminate	0.20046	0.8939	0.94216
Pyridoxamine phosphate	0.19318	0.89885	0.94627
Ectoine	0.18538	0.90413	0.94793
PS(36:2)	0.18457	0.90467	0.94793
[SP] (3'-sulfo)Galbeta- Cer(d18:1/22:0)	0.18334	0.9055	0.94793
PC(42:5)	0.1801	0.90768	0.94793
3-Ketosphingosine	0.1799	0.90781	0.94793
7-Methyladenine	0.17955	0.90804	0.94793
PC(P-36:2)	0.17811	0.90901	0.94793
Proclavaminic acid	0.17804	0.90905	0.94793
Bendiocarb	0.17297	0.91244	0.94793
PS(42:4)	0.17288	0.9125	0.94793
2-Methylcitrate	0.16832	0.91553	0.94793
porphyrin-ring	0.16728	0.91622	0.94793
Hexanoic acid	0.16673	0.91658	0.94793
SM(d18:1/24:1(15Z))	0.16562	0.91731	0.94793
N-Acetyl-L-glutamate	0.1653	0.91753	0.94793
PE(P-36:2)	0.16516	0.91762	0.94793
Phosphonoacetaldehyde	0.16402	0.91837	0.94793
Miserotoxin	0.15802	0.92231	0.9498
UDP-glucuronate	0.15765	0.92255	0.9498
DG(38:6)	0.15641	0.92336	0.9498
2-Aminomalonate semialdehyde	0.15452	0.92459	0.94998
CL(18:2(9Z,12Z)/18:2(9Z,12Z) /18:2(9Z,12Z)/16:1(9Z))	0.14313	0.93195	0.95585
Methylimidazoleacetic acid	0.14222	0.93252	0.95585

Ile-Lys-Ser	0.14069	0.9335	0.95585
2-oxobut-3-enanoate	0.13848	0.9349	0.9562
methiin	0.13505	0.93707	0.95733
cis-Aconitate	0.1319	0.93906	0.95827
Linamarin	0.12701	0.94211	0.96013
5-Hydroxypentanoate	0.12553	0.94302	0.96013
PS(42:8)	0.11895	0.94707	0.96178
Isovalerylcarnitine	0.11867	0.94724	0.96178
Cyanidin 3,5,3'-tri-O-glucoside	0.11765	0.94786	0.96178
L-threo-isocitrate	0.11568	0.94905	0.96191
1-(8-[5]-ladderane-octanoyl)-2-(8-[3]-ladderane-octanyl)- sn-glycerol	0.093947	0.96181	0.9728
[SP amino(18:0/2:0)] 2S-aminooctadecane-1,3R-diol	0.092768	0.96248	0.9728
3-Cyano-L-alanine	0.09176	0.96305	0.9728
Methacholine	0.086838	0.9658	0.97448
[PE(18:0/22:6)] 1-octadecanoyl-2-(4Z,7Z,10Z,13Z,16Z,19Z-docosahexaenoyl)-sn-glycero-3-phosphoethanolamine	0.083936	0.96739	0.97499
PE(P-38:4)	0.073392	0.97303	0.97957
3-Methylamino-L-alanine	0.07038	0.97458	0.98004
penem CGP31608	0.05592	0.98171	0.9861
6-methyl-H2-pterin	0.050842	0.98405	0.98735
Imidazole-4-acetate	0.038771	0.98923	0.99061
N-Formyl-L-aspartate	0.038103	0.9895	0.99061

Stearoylcarnitine	0.012229	0.99803	0.99803

Table S4: List metabolites with significantly different relative abundance from hippocampal tissue of Selenate treated animals.

Metabolite	**F value**	**P value**	**FDR**	**PubChem ID**
PA(40:2)	41.19	2.84E-06	0.0025001	52929451
OH-24:0)	27.385	2.11E-05	0.0092941	5459389
N-Acetyl-D-mannosaminolactone	23.195	4.65E-05	0.013632	440115
PIPES	18.395	0.00013524	0.029753	79723
PC(42:5)	16.474	0.00022147	0.038978	52923145
CL(20:2(11Z,14Z)/18:2(9Z,12Z)/18 :2(9Z,12Z)/18:2(9Z,12Z))	15.394	0.00029834	0.043757	53480396